# THSR states in nuclei and hypernuclei

船木 靖郎

（理研、仁科センター）

*RCNP研究会「核子・ハイペロン多体系におけるクラスター現象」*
*@KGUメディアセンター, 2013年7月26日-27日*

# ``THSR states''

THSR 模型 (mean-field & container描像に基づく)で良く記述される状態

- Gas-like cluster states

  8Be, 12C(Hoyle), 16O(6th 0+)

- Non-gas-like cluster states

  20Ne (inversion doublet bands), （12C(g.s.))

  12C(one dim. linear chain (4th 0+))

  16O(alpha+12C)??

- gas-like cluster states + Λ particle

## ``THSR states''

THSR 模型 (mean-field & container描像に基づく)で良く記述される状態

- Gas-like cluster states

8Be, 12C(Hoyle), 16O($6^{th}$ 0+)

- Non-gas-like cluster states

20Ne (inversion doublet bands), (12C(g.s.))

12C(one dim. linear chain ($4^{th}$ 0+)) 16O(alpha+12C)??

- gas-like cluster states + Λ particle

# Theoretical description

**Particle number projected BCS w.f.**

$$\langle \boldsymbol{r}_1, \cdots, \boldsymbol{r}_{2n} | \mathrm{BCS} \rangle = \mathcal{A}\Big\{ \Phi(\boldsymbol{r}_1, \boldsymbol{r}_2)\Phi(\boldsymbol{r}_3, \boldsymbol{r}_4)\cdots\Phi(\boldsymbol{r}_{2n-1}, \boldsymbol{r}_{2n}) \Big\}$$

**n α condensate w.f.**

$$\langle \boldsymbol{r}_1, \cdots, \boldsymbol{r}_{4n} | \Phi_{n\alpha} \rangle = \mathcal{A}\Big\{ \Phi(\boldsymbol{r}_1, \boldsymbol{r}_2, \boldsymbol{r}_3, \boldsymbol{r}_4)\Phi(\boldsymbol{r}_5, \boldsymbol{r}_6, \boldsymbol{r}_7, \boldsymbol{r}_8)\cdots\Phi(\boldsymbol{r}_{4n-3}, \boldsymbol{r}_{4n-2}, \boldsymbol{r}_{4n-1}, \boldsymbol{r}_{4n}) \Big\}$$

**Variational ansatz (two parameters B and b)**

(THSR ansatz) A. Tohsaki, H. Horiuchi, P. Schuck and G. Röpke et al., PRL 87, 192501 (2001).

$$\Phi(\boldsymbol{r}_{4i-3}, \cdots, \boldsymbol{r}_{4i}) = e^{-\frac{2}{B^2}(\boldsymbol{X}_i - \boldsymbol{X}_G)^2} \phi_\alpha(\boldsymbol{r}_{4i-3}, \cdots, \boldsymbol{r}_{4i})$$

$$\phi_\alpha \propto e^{-\frac{1}{8b^2}\sum_{k<l}(\boldsymbol{r}_k - \boldsymbol{r}_l)^2}$$

c.o.m. of *i*-th α particle

$$\boldsymbol{X}_i = \frac{\boldsymbol{r}_{4i-3} + \cdots + \boldsymbol{r}_{4i}}{4}$$

Total c.o.m.

$$\boldsymbol{X}_G = \frac{\boldsymbol{r}_1 + \cdots + \boldsymbol{r}_{4n}}{4n}$$

**n=3 case**

$$\Phi_{3\alpha}(B, b) =$$

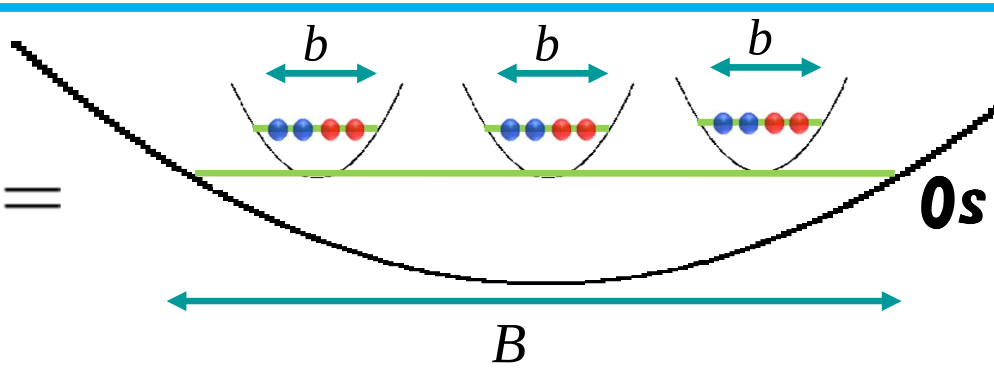


$$\phi_\alpha(\boldsymbol{r}_1, \cdots, \boldsymbol{r}_4) \doteq$$

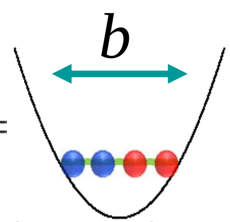


$(0s)^4$ configuration

**Two limits**

**B = b: Shell model w.f.**

**B >> b: Gas of independent α-particles**

# Inversion doublet rotational bands in $^{20}$Ne

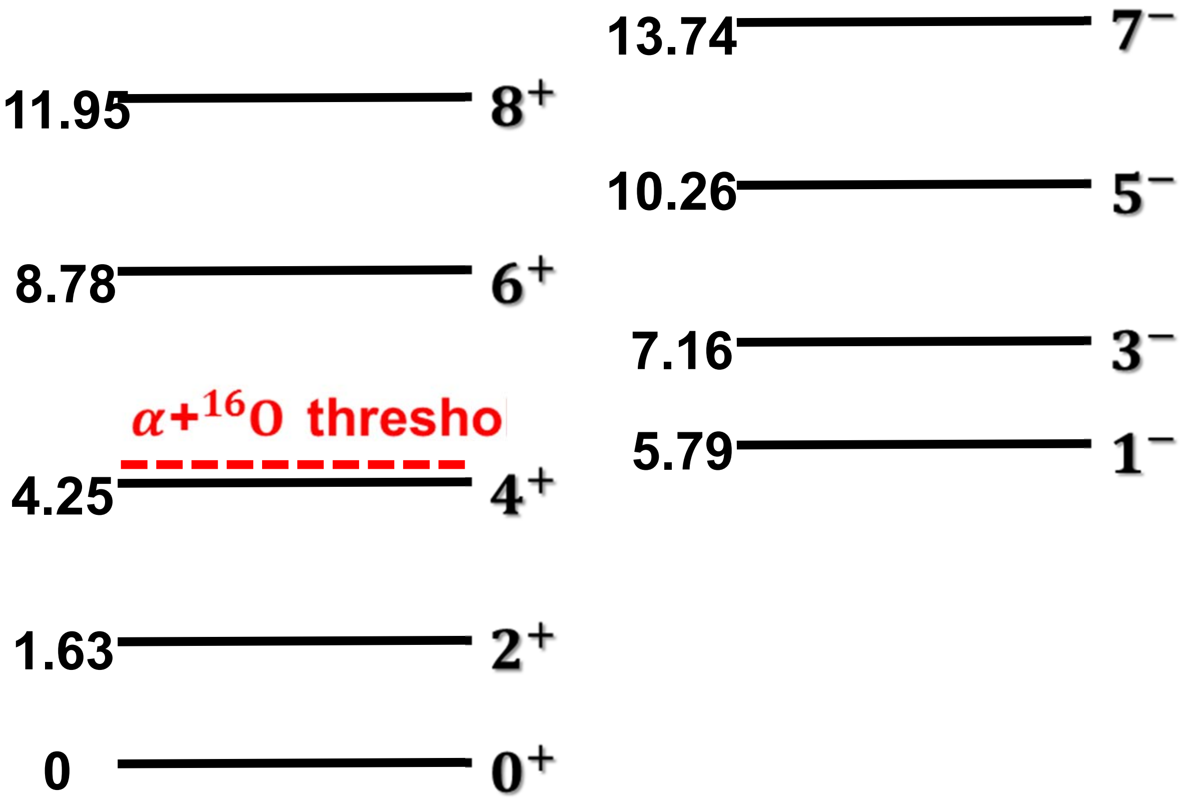


$K^{\pi} = 0_1^{+}$

$K^{\pi} = 0_1^{-}$

**Mixture of shell and cluster**

**The well-developed cluster structure**

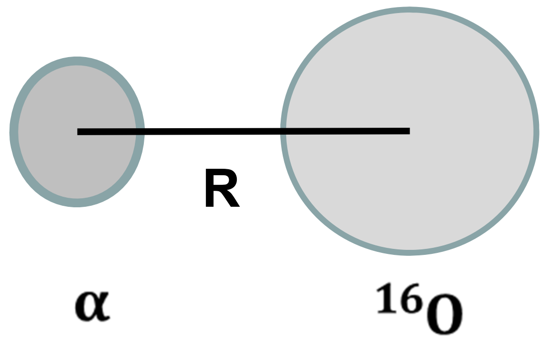


**The inversion doublet bands provide a very typical case for testing whether or not the THSR idea can be extended to the general cluster structures.**

# Model wave functions of $^{20}$Ne

$$\Psi_{\mathrm{Ne}}(\boldsymbol{\beta}, \boldsymbol{S}) = \boxed{\exp\left(-\frac{10X_G^2}{b^2}\right)\mathscr{A}\left[\exp\left(-\sum_{k}^{x,y,z}\frac{8(\boldsymbol{r}-\boldsymbol{S})_k^2}{5B_k^2}\right)\phi(\alpha)\phi(^{16}\mathrm{O})\right]}$$

## Hybrid THSR w.f

- B = b, S > 0 : Brink (localized) w.f.
- B > b, S = 0 : THSR(parametrized by density, cluster occupying an orbit)
- B = b, S = 0 : harmonic oscillator w.f.

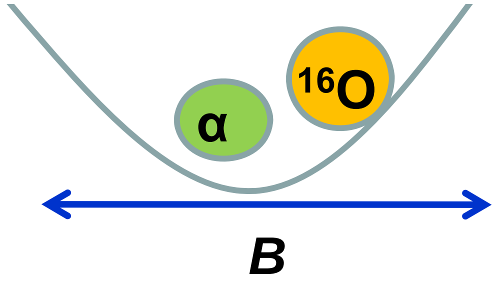


## Brink (localized) w.f

$$\Phi^{B}_{\mathrm{Ne}}\left(\frac{4}{5}\boldsymbol{R}, -\frac{1}{5}\boldsymbol{R}\right) \propto \exp\left(-\frac{10X_G^2}{b^2}\right)\mathscr{A}\left[\exp\left(-\frac{8(\boldsymbol{r}-\boldsymbol{R})^2}{5b^2}\right)\phi(\alpha)\phi(^{16}\mathrm{O})\right]$$

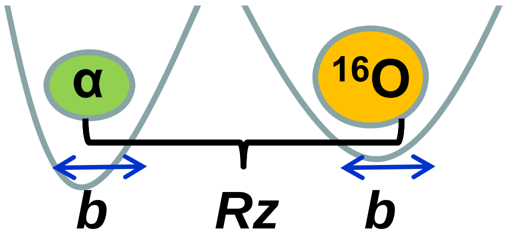


(traditional microscopic cluster model)

Where $r = X_1 - X_2$, and $\phi(\alpha)$ and $\phi(^{16}\mathrm{O})$ represent the intrinsic harmonic oscillator shell-model wave functions of alpha cluster and $^{16}$O cluster, respectively.

# The localized concept in Brink model

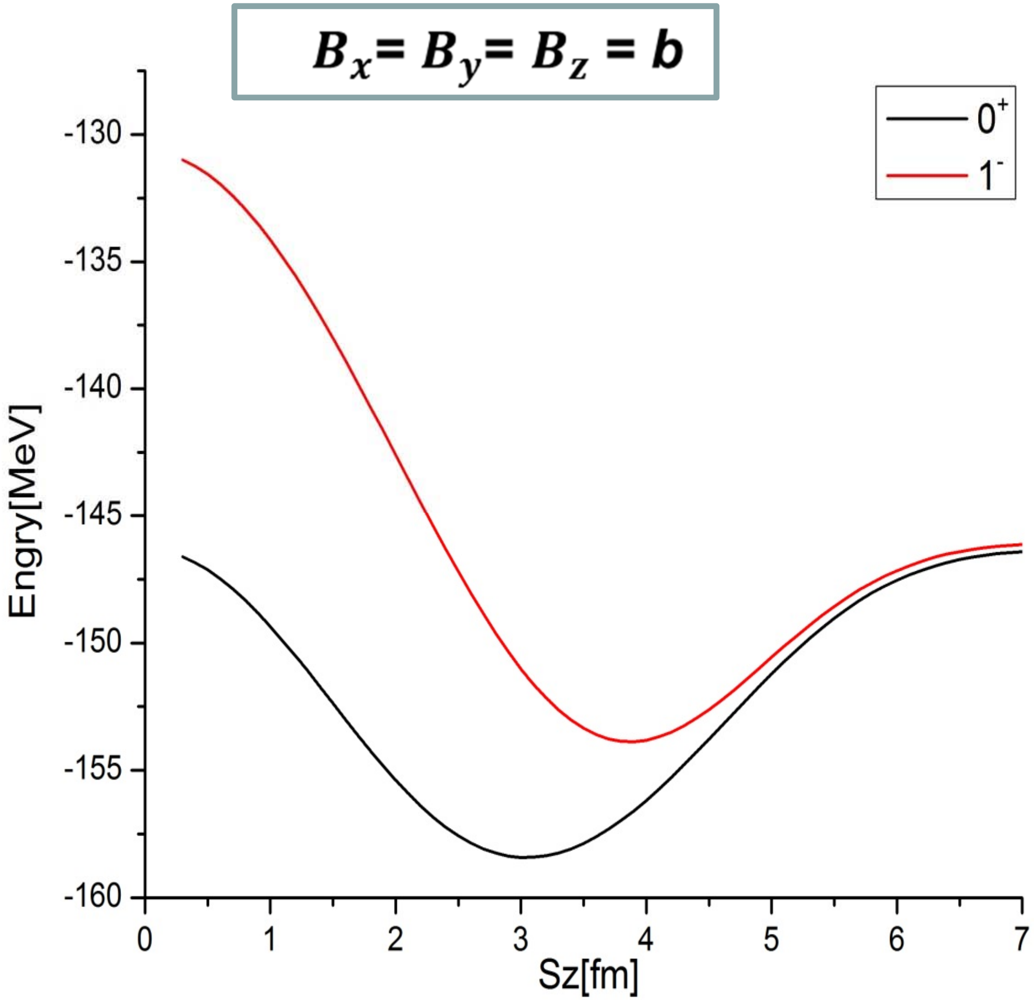


The non-zero value Sz
the localized clustering.

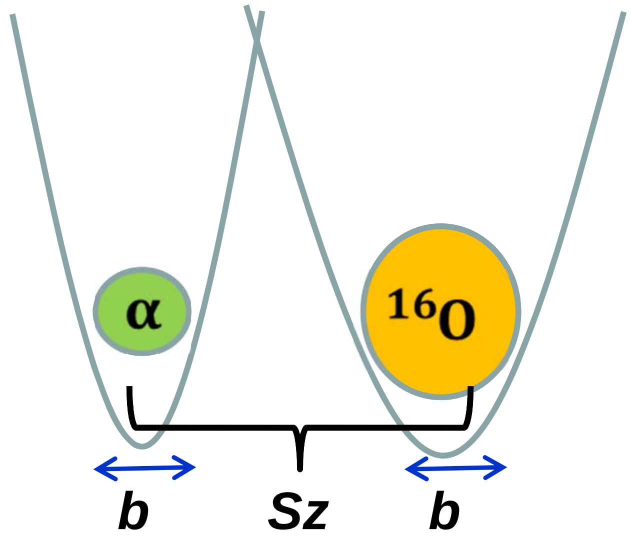


**Sz is the inter-cluster distance parameter in Brink model.**

# The localized concept in Brink model

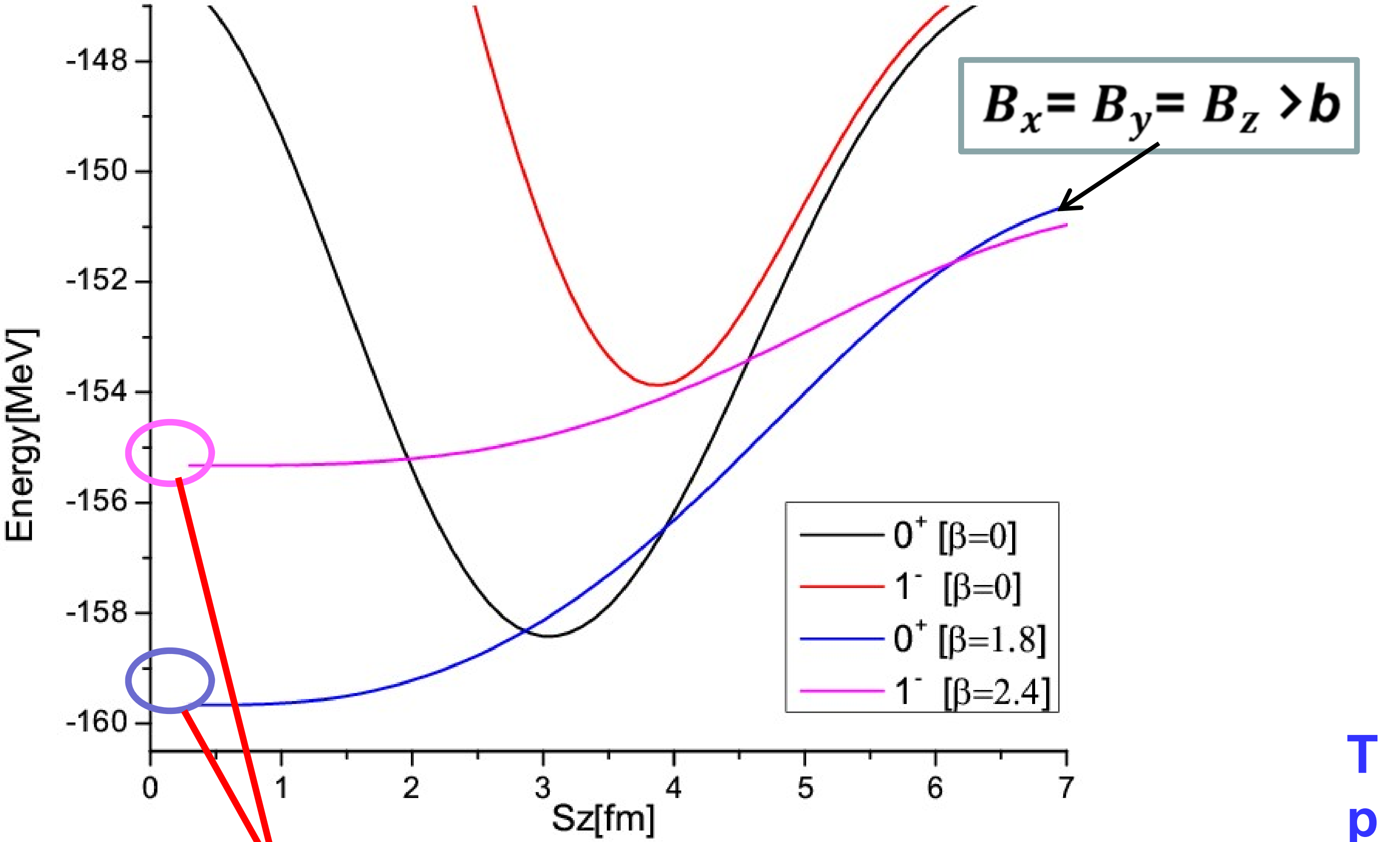


non- localized clustering !

The non-zero value Sz
the localized clustering.

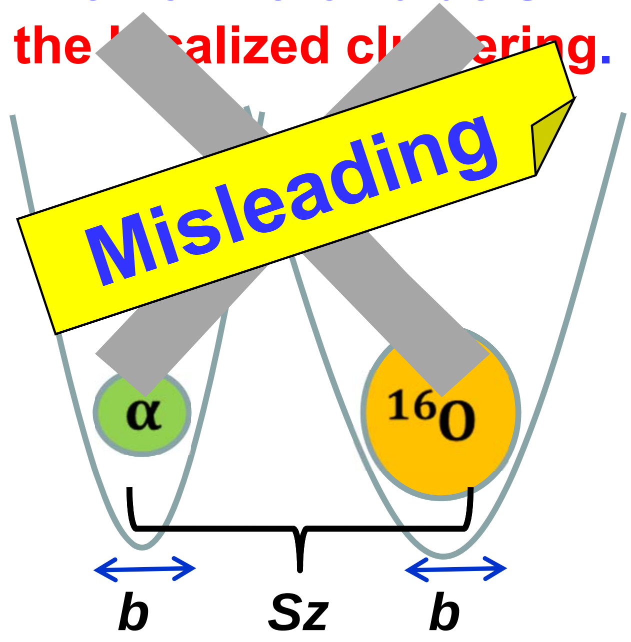


The localized (from Pauli principle ) and non-localized.
Cluster orbit is generated.

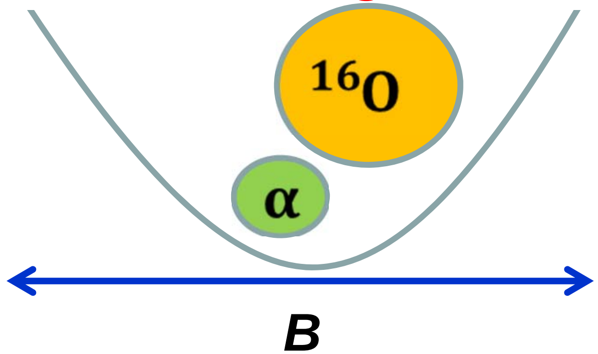


$b$=1.46 fm → Bx=By=Bz=2.93 fm for $0^+$.
→ Bx=By=Bz=3.69 fm for $1^-$.

*Further demonstrating the advantage and usefulness of THSR,*

# The energy levels of α+$^{16}$O inversion doublet bands in $^{20}$Ne by THSR w.f.

*B. Zhou, Y. F. et al., PRC86, 014301 (2012); PRL110, 262501(2013).*

In parentheses

$$\left|\left\langle \Psi^{\mathrm{THSR}}_{\mathrm{single}} \,\middle|\, \Phi^{\alpha+^{16}\mathrm{O\ Brink}}_{\mathrm{GCM}} \right\rangle\right|^2$$

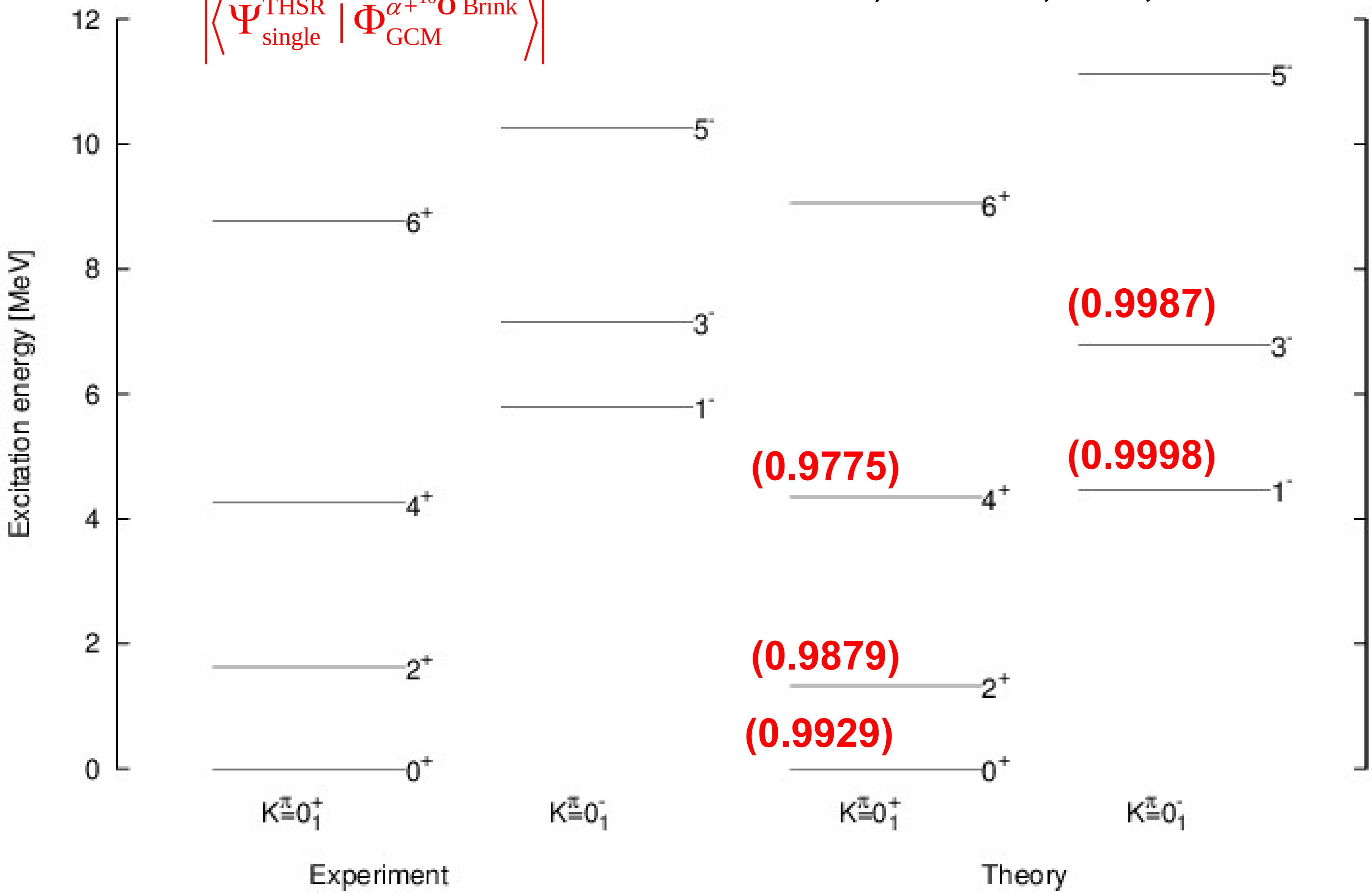


**The rotational bands are reproduced using the single THSR w.fs.**

# Alpha clusters in light hypernuclei using Hyper-THSR w.f.

Y. Funaki, T. Yamada, E. Hiyama, K. Ikeda

# Model

- $\alpha$ condensate type wave function (THSR)
- fully microscopic model

A. Tohsaki et al., PRL 87, 192501 (2001).

- only one parameter, $B$ (with deformation, $B_x$ ,$B_y$ ,$B_z$)
  which characterizes nuclear density

$$\Phi_{3\alpha}^{THSR}(B) = \mathcal{A}$$

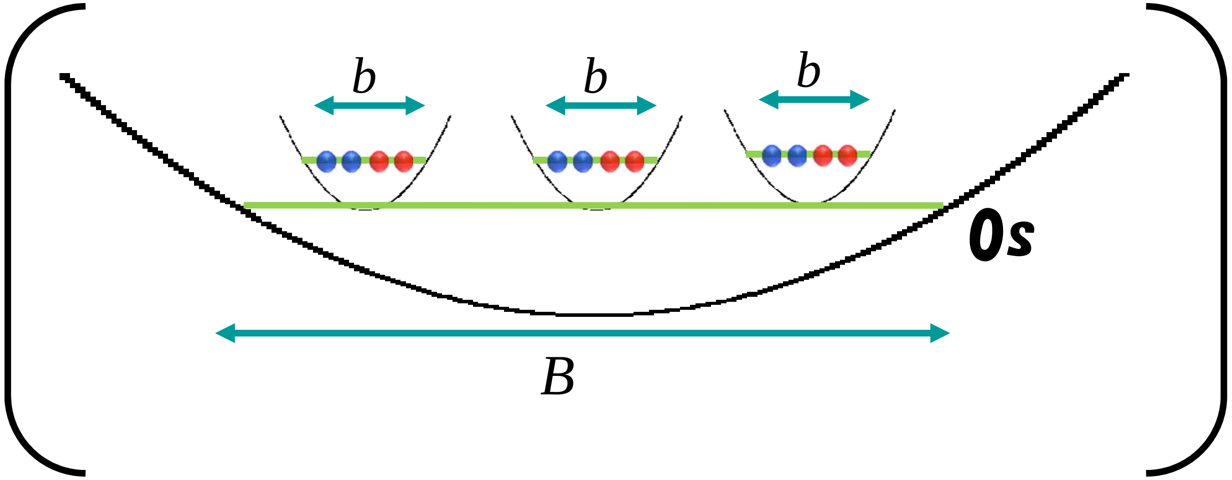


$B \sim b$: ground state
$B >> b$ : $\alpha$ condensed state

$b$ : fixed at a size of $\alpha$ particle in free space

*Spatial shrinkage happens when $\Lambda$ particle is injected in a nucleus.*
*The corresponding rearrangement effect can be optimally described.*

# Hyper-THSR, applied to $^{9}{}_{\Lambda}$Be, $^{13}{}_{\Lambda}$C, $^{17}{}_{\Lambda}$O, …

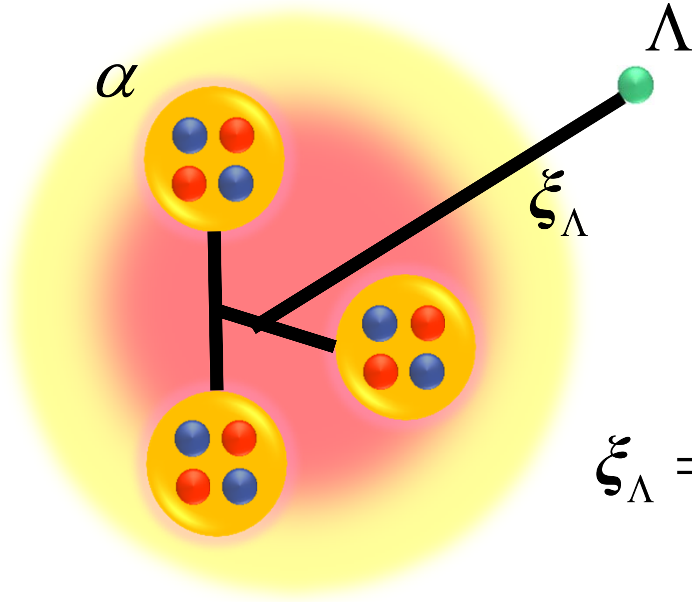


**Λ particle is a good probe to investigate the analogous states to ordinary nuclei.**

- ***out of antisymmetrization of nucleons***
- ***glue-like role***

$$\xi_\Lambda = \boldsymbol{r}_\Lambda - \boldsymbol{X}_C \quad \boldsymbol{X}_C = \frac{\boldsymbol{r}_1 + \cdots + \boldsymbol{r}_{4n}}{4n}$$

$\hat{\mathcal{P}}_I$: angular momentum projection operator

$$\Phi^{\text{Hyper-THSR}}_{[I,l]_J}(B_\perp, B_z, \kappa) = \mathcal{A}\left\{\prod_{i=1}^{n} \hat{\mathcal{P}}_I \chi^{THSR}_{3\alpha}(B_\perp, B_z : \boldsymbol{X}_i - \boldsymbol{X}_C)\phi(\alpha_i)\right\}\varphi^{(l)}_\kappa(\xi_\Lambda)$$

$$\chi^{\text{THSR}}(\boldsymbol{X} : B_\perp, B_z) = \exp\left(-\frac{2}{B_\perp^2}(X_x^2 + X_y^2) - \frac{2}{B_z^2}X_z^2\right)$$

$$\varphi^{(l)}_\kappa(\xi_\Lambda) = N_{\kappa,l}\xi_\Lambda{}^l \exp\left(-\frac{\xi_\Lambda^2}{\kappa^2}\right) Y_{lm}(\hat{\xi}_\Lambda)$$

**In the present study, $l$=0 only taken into account**

**Validity of this model should be checked.**

**Application to $^{13}{}_{\Lambda}$C**

# 3α+Λ OCM by Hiyama et al.

YNG (JA) interaction

E. Hiyama et al., PTP 97, 881 (1997).

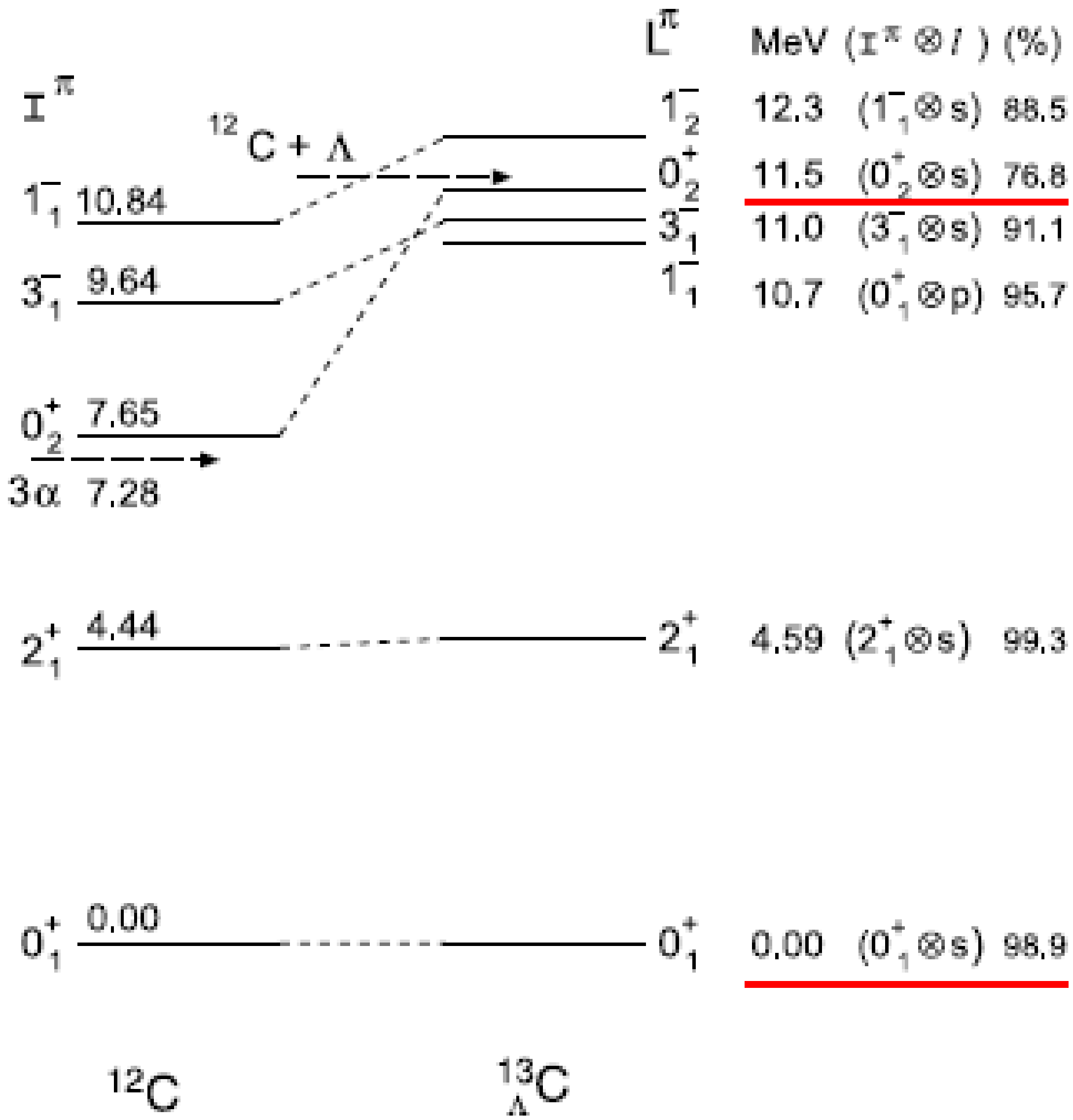


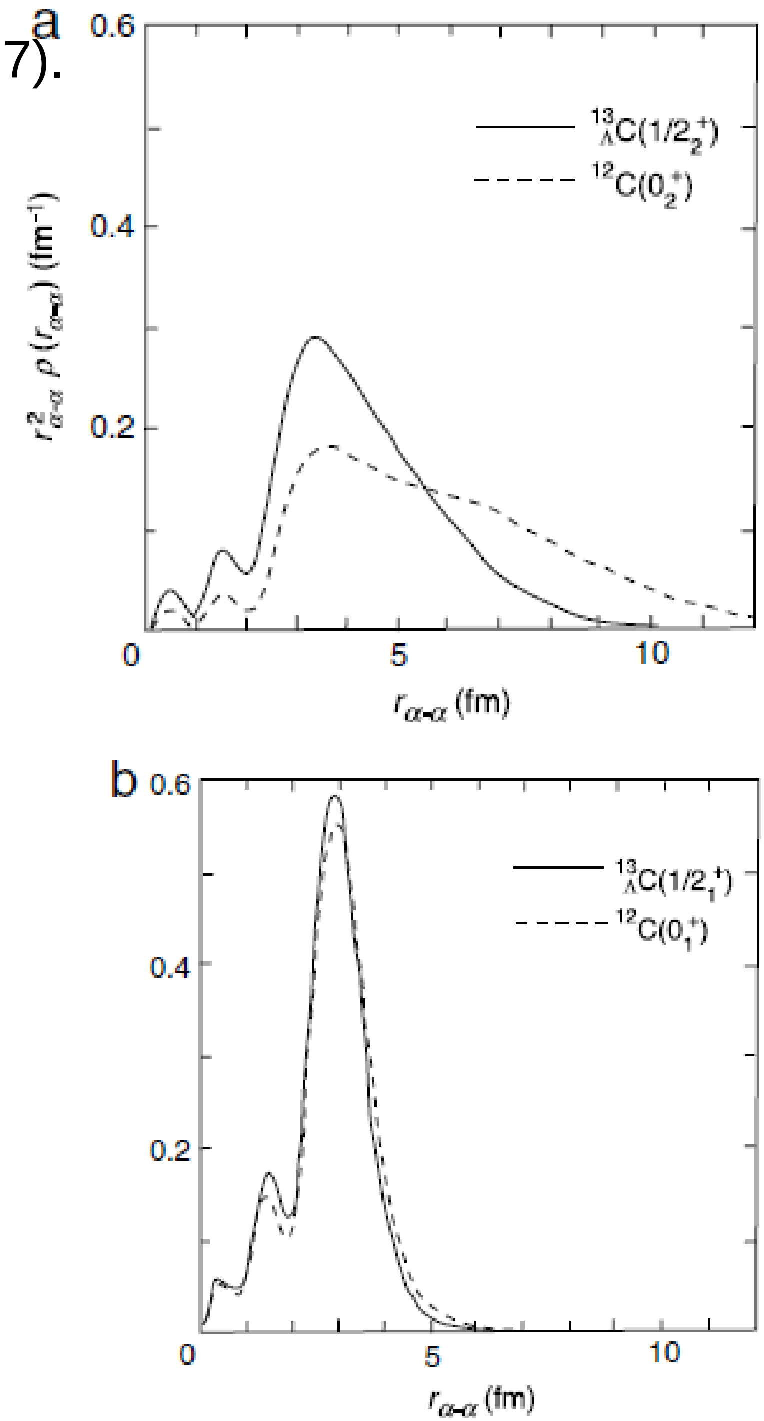


Spatial shrinkage is seen.

# Energy of $^{13}{}_{\Lambda}C(0^+)$

•Hyper-THSR gives better results than RGM+Λ.

$$\sum_{B'_\perp, B'_z, \kappa'} \left\langle \Phi^{\text{Hyper-THSR}}_{[0,0]_0}(B_\perp, B_z, \kappa) \middle| H - E_\lambda \middle| \Phi^{\text{Hyper-THSR}}_{[0,0]_0}(B'_\perp, B'_z, \kappa') \right\rangle f_\lambda(B'_\perp, B'_z, \kappa') = 0$$

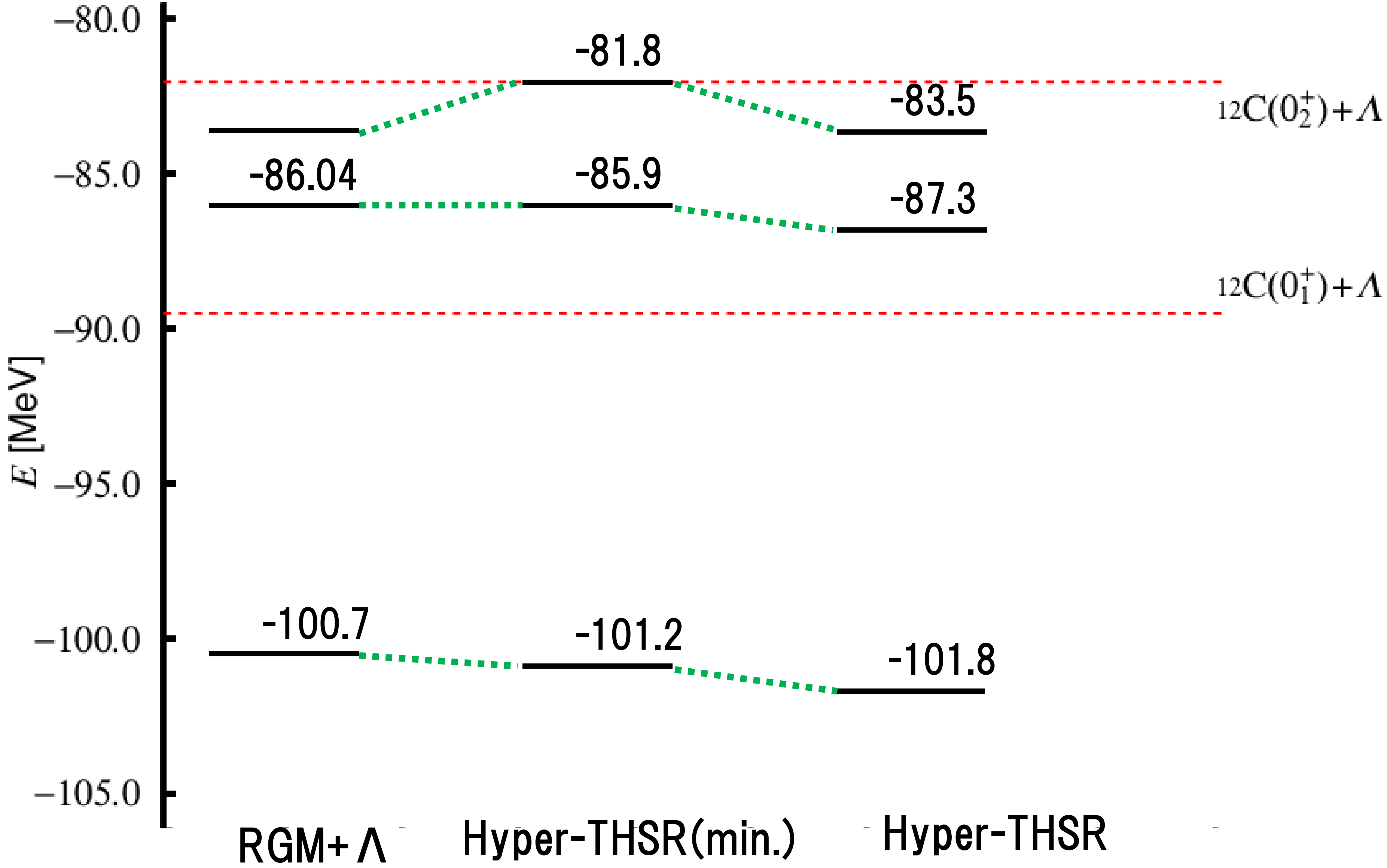


RGM+Λ: Yamada et al., PTPS 81, (1985)

# ${}^{9}_{\Lambda}$Be($0^+$,$2^+$, $4^+$) Energy spectra & squared overlap

$$O(\beta_\perp,\beta_z,\kappa)=\left|\sum_{B'_\perp,B'_z}\left\langle \Phi^{\text{Hyper-THSR}}_{[J,0]_J}(B_\perp,B_z,\kappa)\middle|\Phi^{\text{Hyper-THSR}}_{[J,0]_J}(B'_\perp,B'_z,\kappa)\right\rangle f_\lambda(B'_\perp,B'_z,\kappa)\right|^2$$

$$\sum_{B'_\perp,B'_z}\left\langle \Phi^{\text{Hyper-THSR}}_{[0,0]_0}(B_\perp,B_z,\kappa)\middle|H-E_\lambda(\kappa)\middle|\Phi^{\text{Hyper-THSR}}_{[0,0]_0}(B'_\perp,B'_z,\kappa)\right\rangle f_\lambda(B'_\perp,B'_z)=0$$

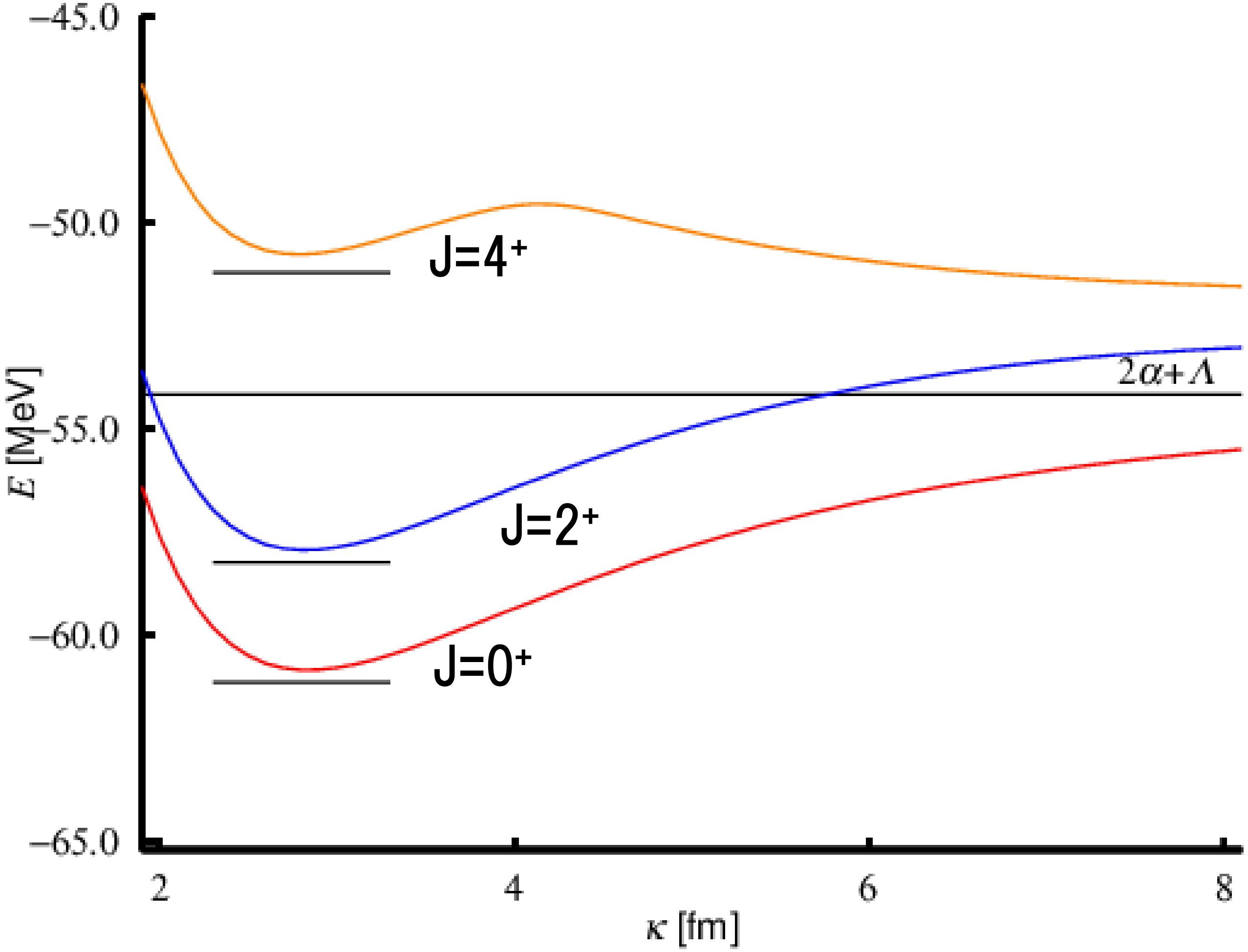


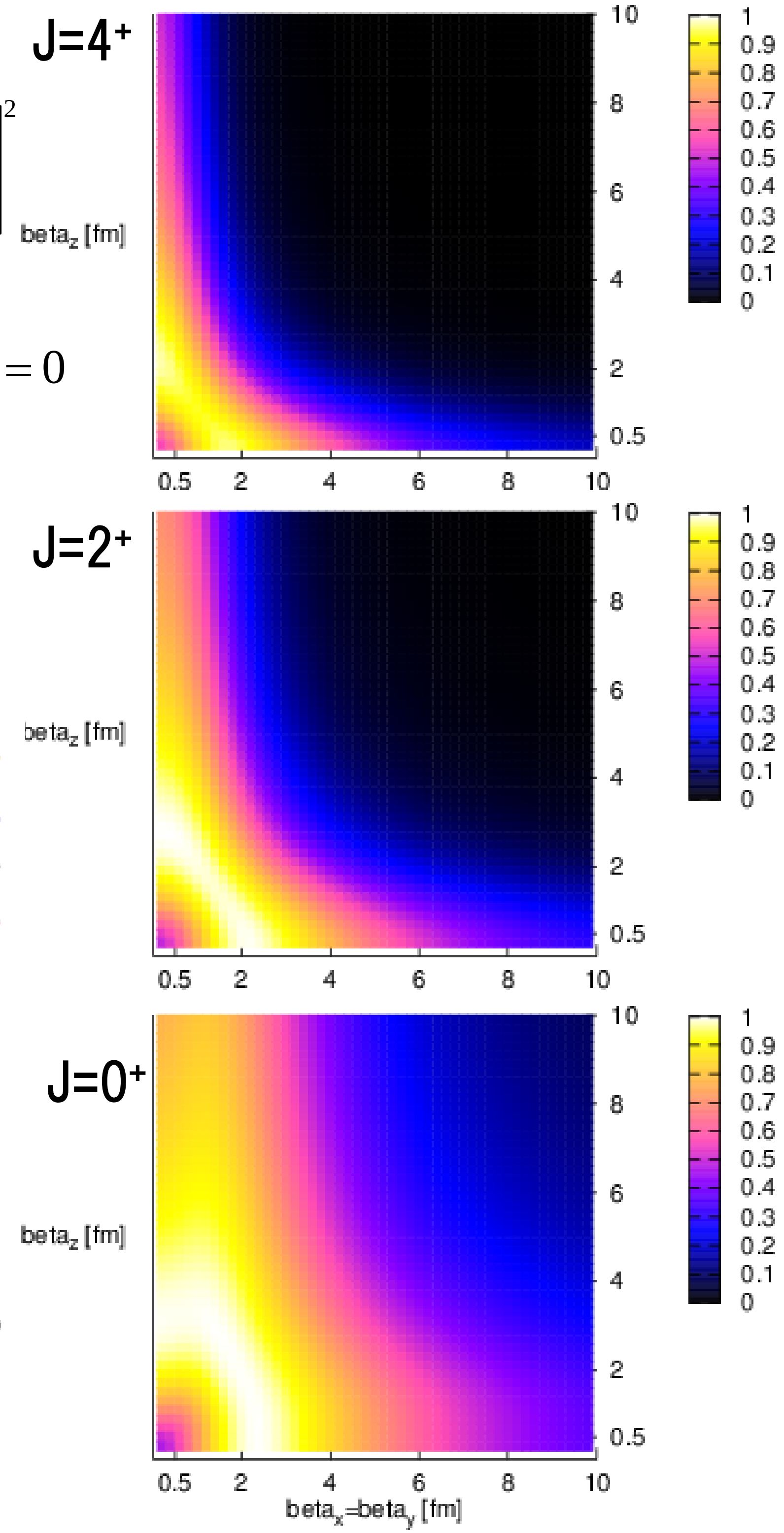

# Comparison of intrinsic density between $^{8}$Be($0^{+}$) & $^{9}{}_{\Lambda}$Be($0^{+}$)

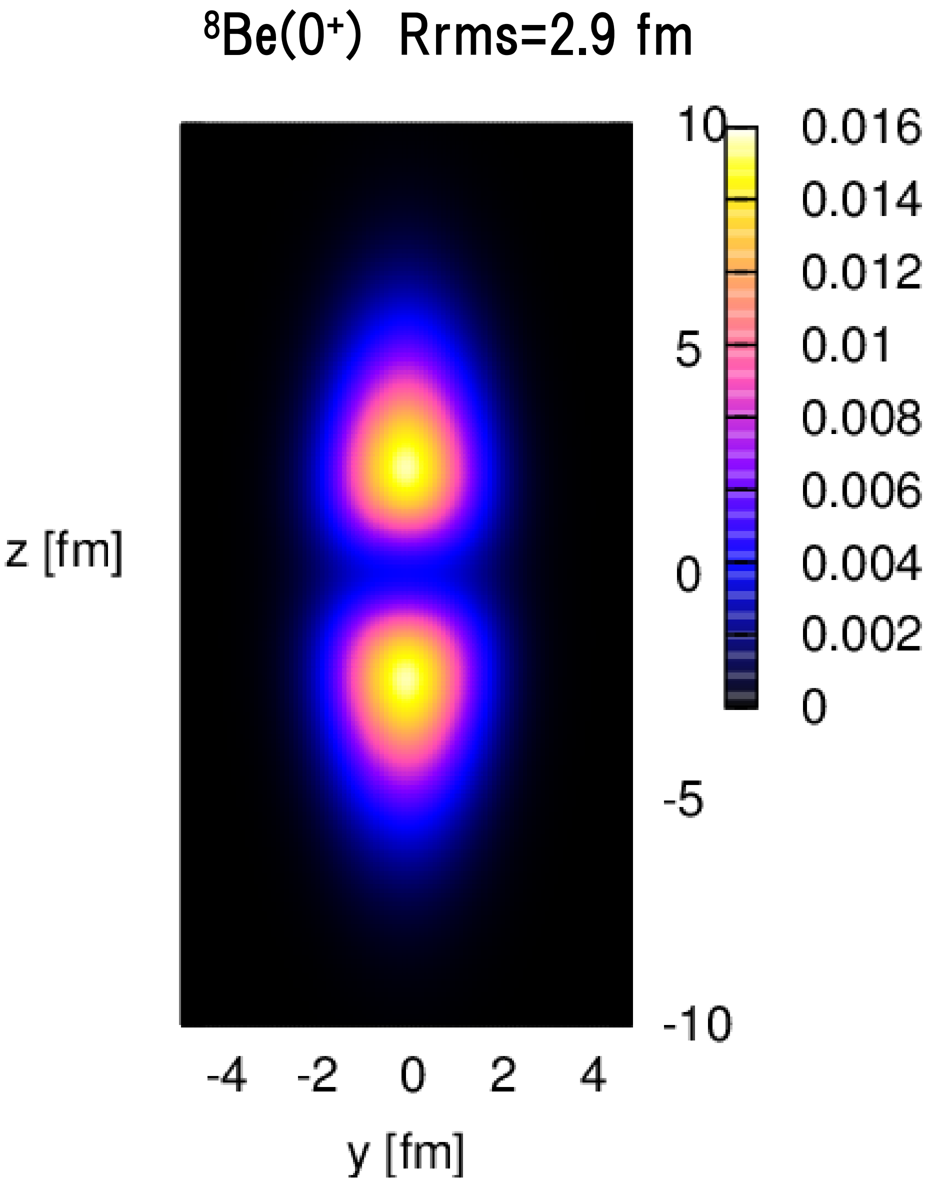


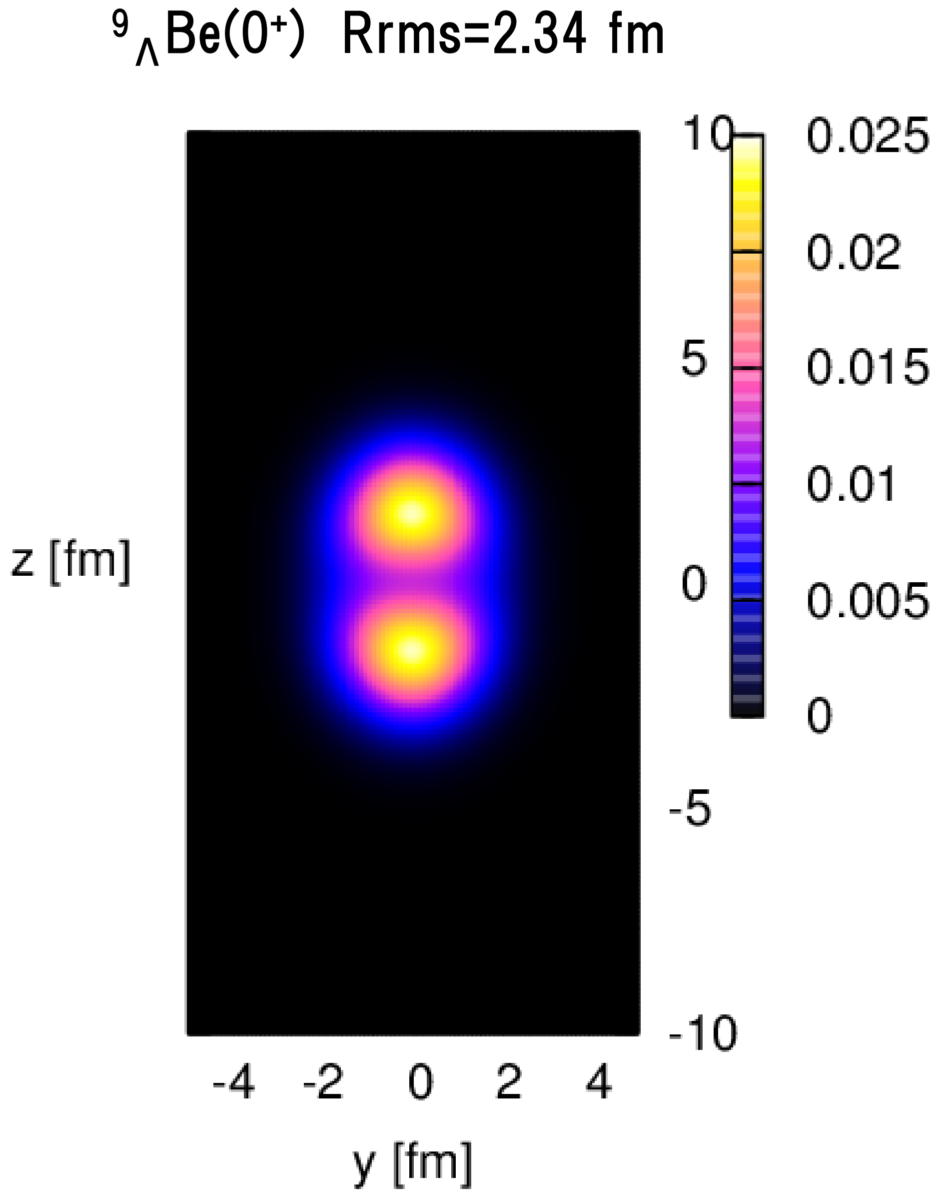

# Energy curve of $^{13}{}_{\Lambda}C(0^+)$ as a function of $\kappa$ YNG (ND) interaction

$$\sum_{B'_\perp, B'_z} \left\langle \Phi^{\text{Hyper-THSR}}_{[0,0]_0}(B_\perp, B_z, \kappa) \middle| H - E_\lambda(\kappa) \middle| \Phi^{\text{Hyper-THSR}}_{[0,0]_0}(B'_\perp, B'_z, \kappa) \right\rangle f_\lambda(B'_\perp, B'_z) = 0$$

$$\Lambda \text{ particle w.f.}: \varphi_\kappa^{(l=0)}(\xi_\Lambda) = N_{\kappa,l=0} \exp\left(-\frac{\xi_\Lambda^2}{\kappa^2}\right) Y_{00}(\hat{\xi}_\Lambda)$$

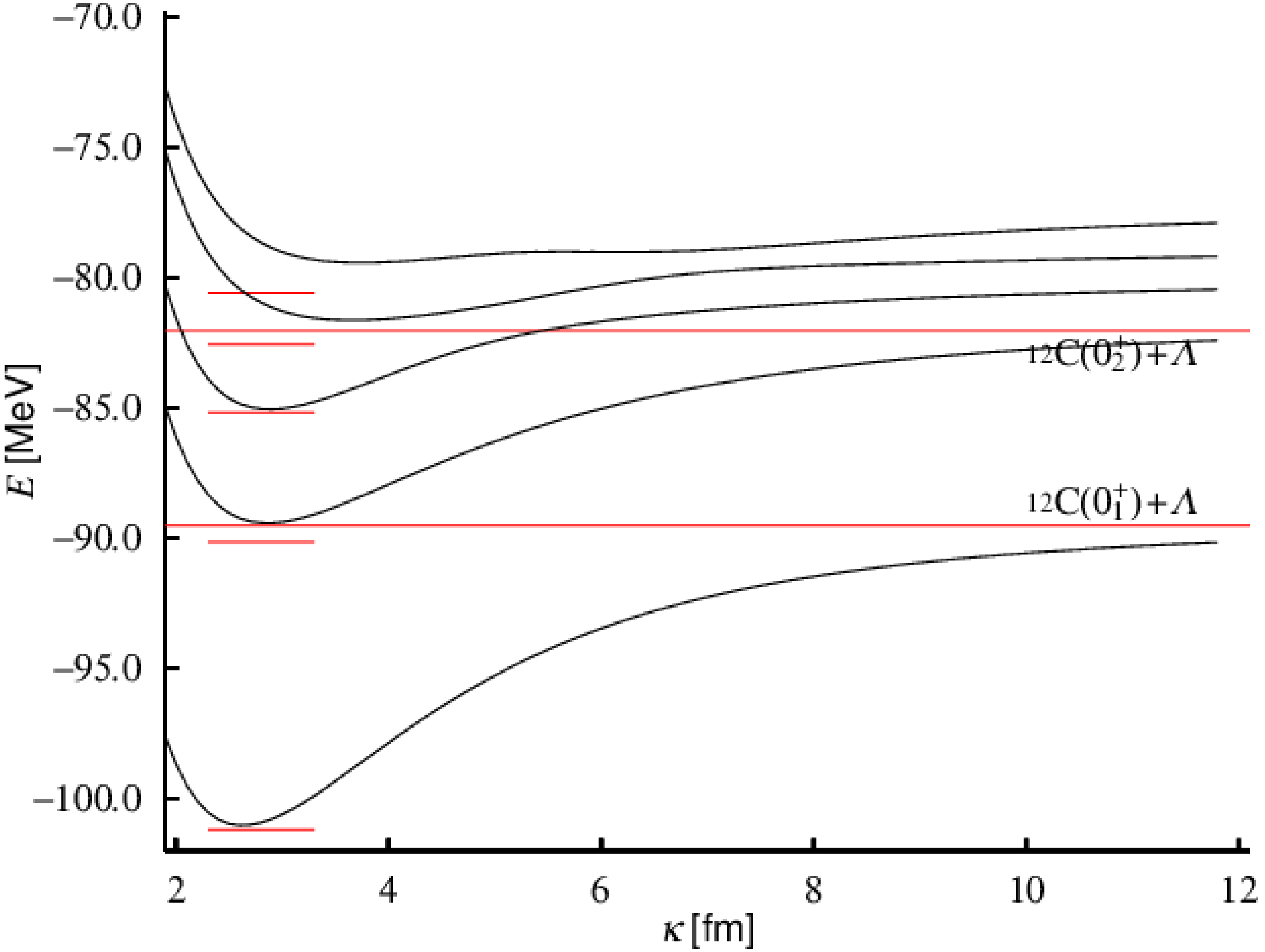


Lowest :
$k_f$=1.135 fm$^{-1}$
Others :
$k_f$=0.962 fm$^{-1}$

# Energy curve of $^{13}{}_{\Lambda}C(2^+)$ as a function of $\kappa$ YNG (ND) interaction

$$\sum_{B'_\perp, B'_z} \left\langle \Phi^{\text{Hyper-THSR}}_{[2,0]_2}(B_\perp, B_z, \kappa) \middle| H - E_\lambda(\kappa) \middle| \Phi^{\text{Hyper-THSR}}_{[2,0]_2}(B'_\perp, B'_z, \kappa) \right\rangle f_\lambda(B'_\perp, B'_z) = 0$$

$$\Lambda \text{ particle w.f.}: \varphi^{(l=0)}_{\kappa}(\xi_\Lambda) = N_{\kappa,l=0} \exp\left(-\frac{\xi_\Lambda^2}{\kappa^2}\right) Y_{00}(\hat{\xi}_\Lambda)$$

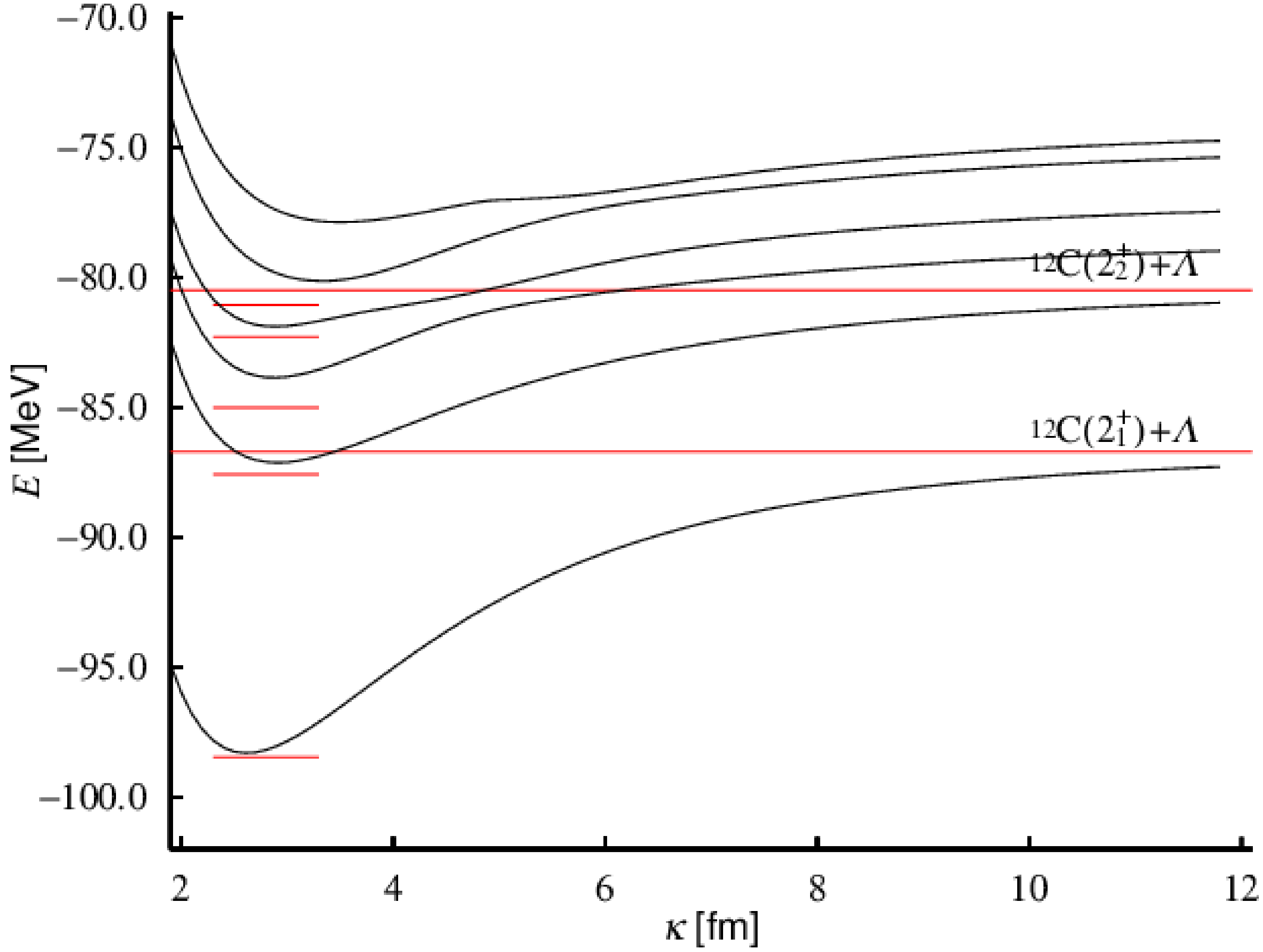


Lowest :
$k_f$=1.135 $fm^{-1}$
Others :
$k_f$=0.962 $fm^{-1}$

# Energy curve of $^{13}{}_{\Lambda}C(4^+)$ as a function of $\kappa$ YNG （ND） interaction

$$\sum_{B'_\perp, B'_z} \left\langle \Phi^{\text{Hyper-THSR}}_{[4,0]_4}(B_\perp, B_z, \kappa) \middle| H - E_\lambda(\kappa) \middle| \Phi^{\text{Hyper-THSR}}_{[4,0]_4}(B'_\perp, B'_z, \kappa) \right\rangle f_\lambda(B'_\perp, B'_z) = 0$$

$$\Lambda \text{ particle w.f.}: \varphi_\kappa^{(l=0)}(\xi_\Lambda) = N_{\kappa,l=0} \exp\left(-\frac{\xi_\Lambda^2}{\kappa^2}\right) Y_{00}\left(\hat{\xi}_\Lambda\right)$$

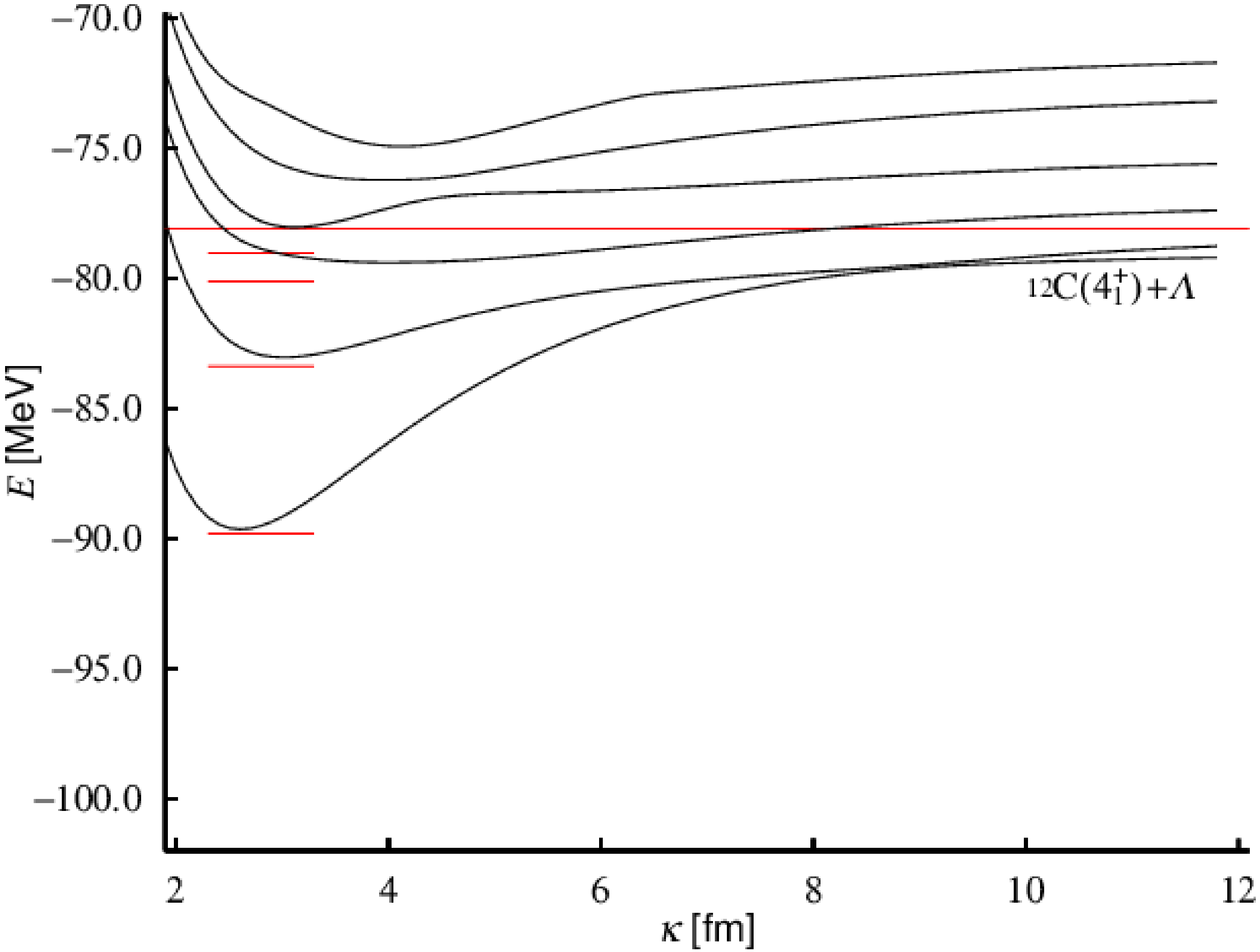


Lowest：
$k_f$=1.135 $fm^{-1}$
Others：
$k_f$=0.962 $fm^{-1}$

# Energy of $^{13}{}_{\Lambda}C(0^+, 2^+, 4^+)$

**YNG (ND) interaction**

$$\sum_{B'_\perp, B'_z, \kappa'} \left\langle \Phi^{\text{Hyper-THSR}}_{[J,0]_J}(B_\perp, B_z, \kappa) \middle| H - E_\lambda \middle| \Phi^{\text{Hyper-THSR}}_{[J,0]_J}(B'_\perp, B'_z, \kappa') \right\rangle f_\lambda(B'_\perp, B'_z, \kappa') = 0$$

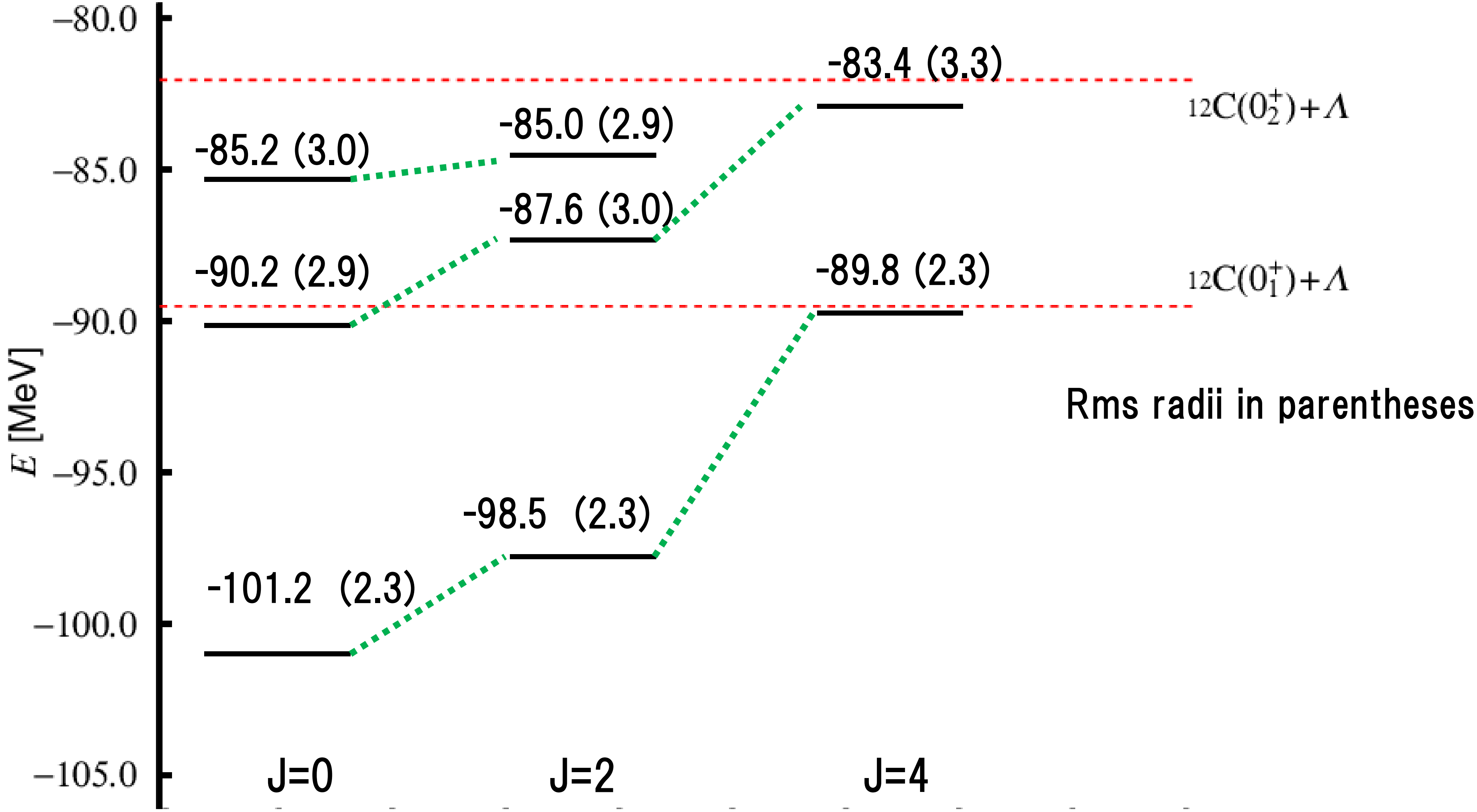

# Size dependence of occupation probability (amount of $\alpha$ condensation)

(Hoyle + Λ)
$R_{rms}$=2.9 fm

Condensate character still much survives.
～60 %

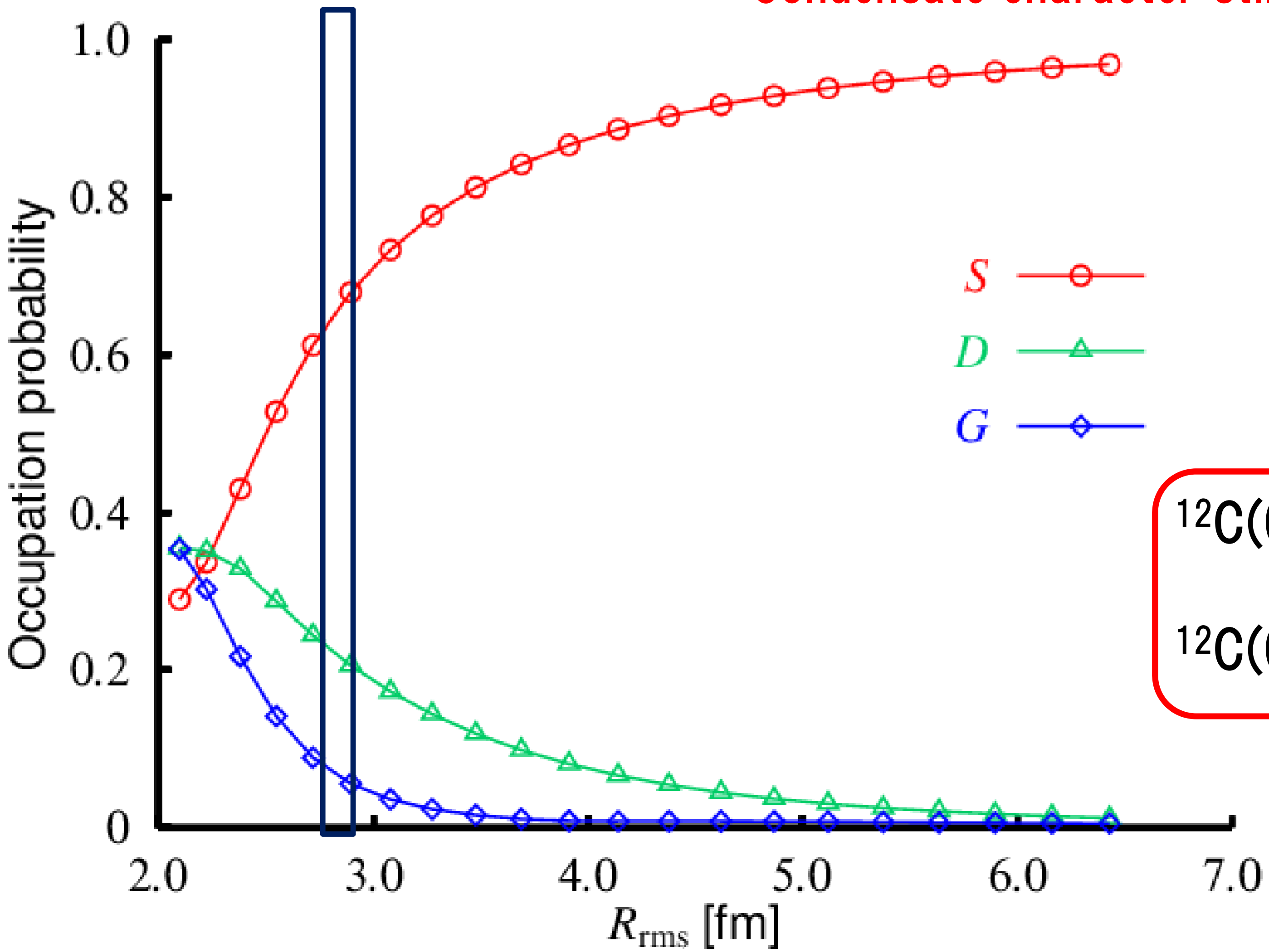


$^{12}C(0_1^+)$ 2.4 fm

$^{12}C(0_2^+)$ 3.8 fm

$R_{rms}$ < 2.5 fm: Alpha's are resolved due to the antisymmetrization.

$R_{rms}$ → large: Alpha's occupy a single *S*-orbit only.

# Squared overlap surfaces for $0_1^+$, $2_1^+$, $4_1^+$

$$O(\beta_\perp, \beta_z, \kappa) = \left| \sum_{B'_\perp, B'_z} \left\langle \Phi^{\text{Hyper-THSR}}_{[J,0]_J}(B_\perp, B_z, \kappa) \middle| \Phi^{\text{Hyper-THSR}}_{[J,0]_J}(B'_\perp, B'_z, \kappa) \right\rangle f_\lambda(B'_\perp, B'_z, \kappa) \right|^2$$

$0_1^+$

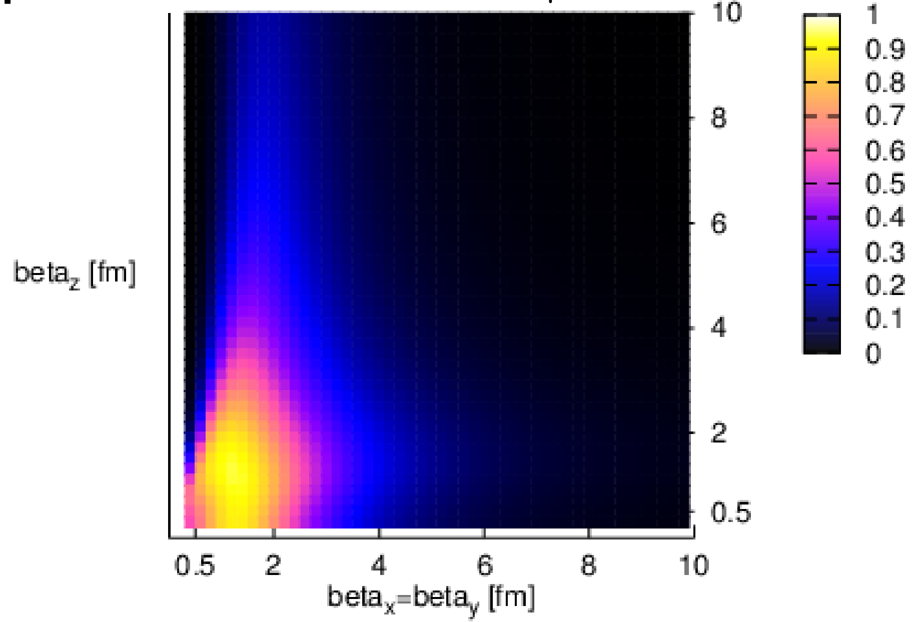


$2_1^+$

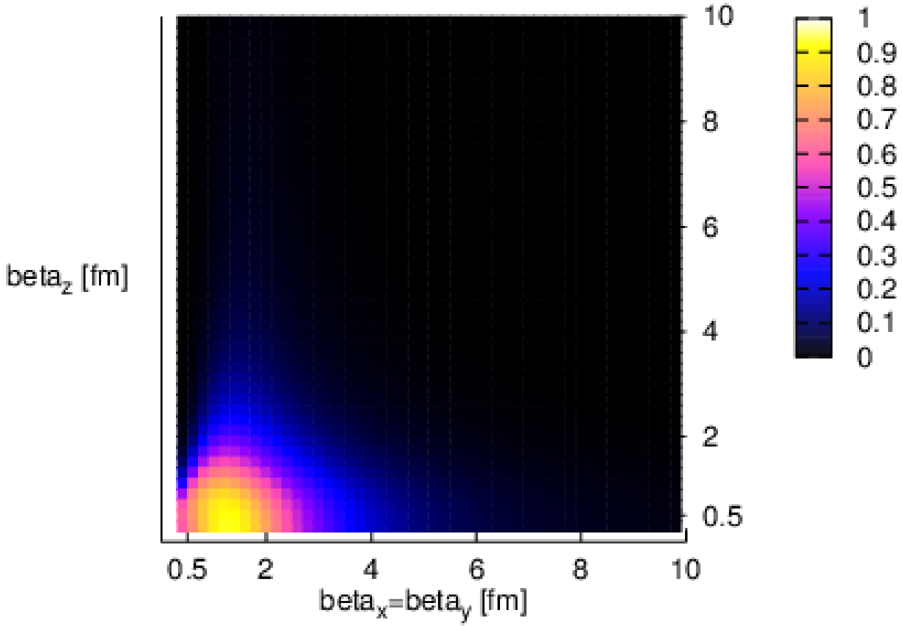


$4_1^+$

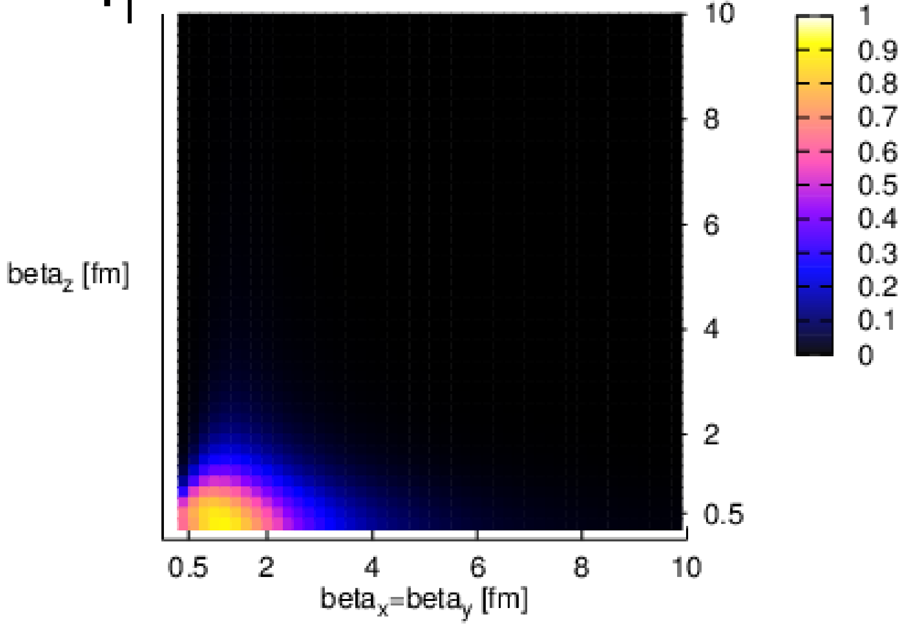

# Family of the Hoyle state

$0_2^+$

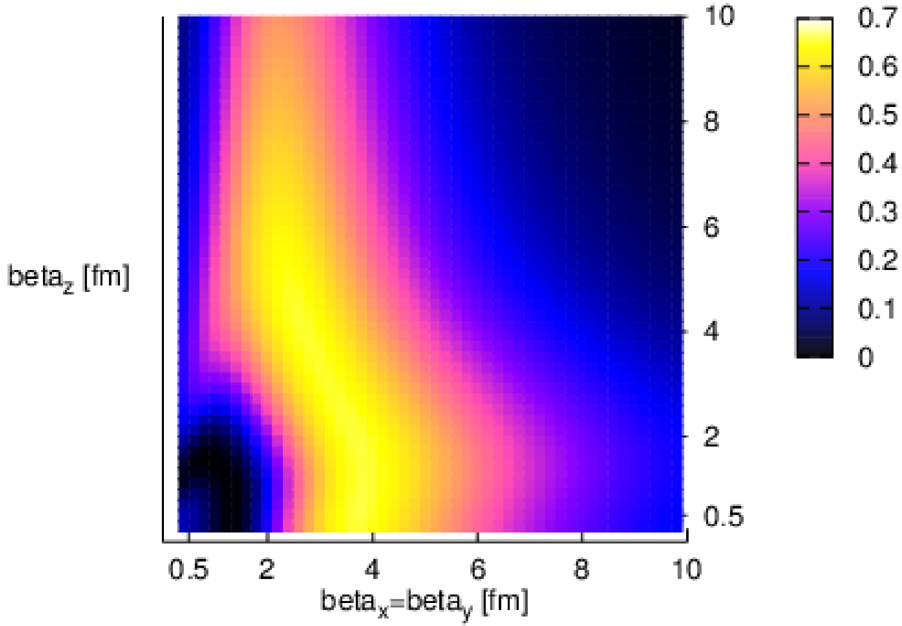


$2_2^+$

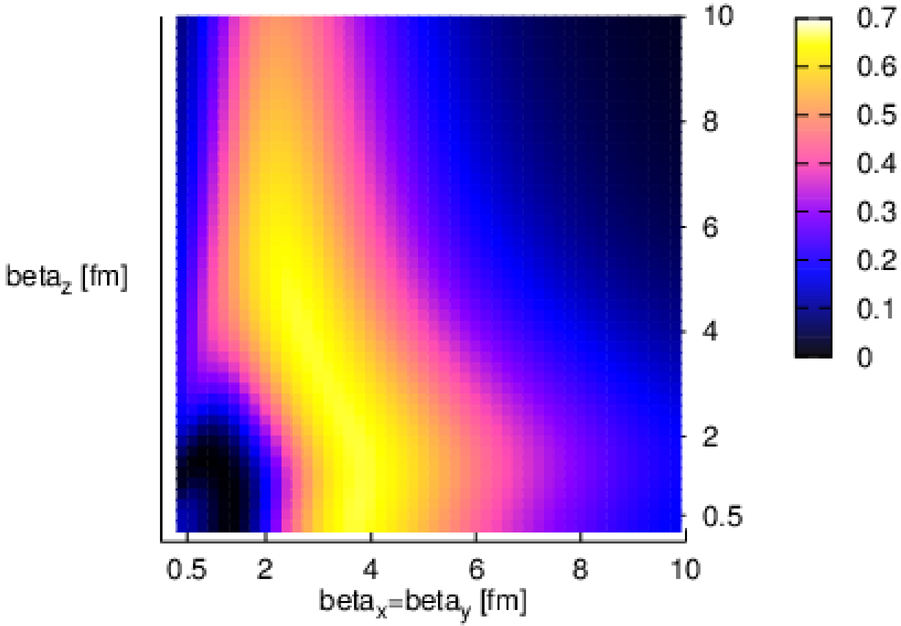


$4_2^+$

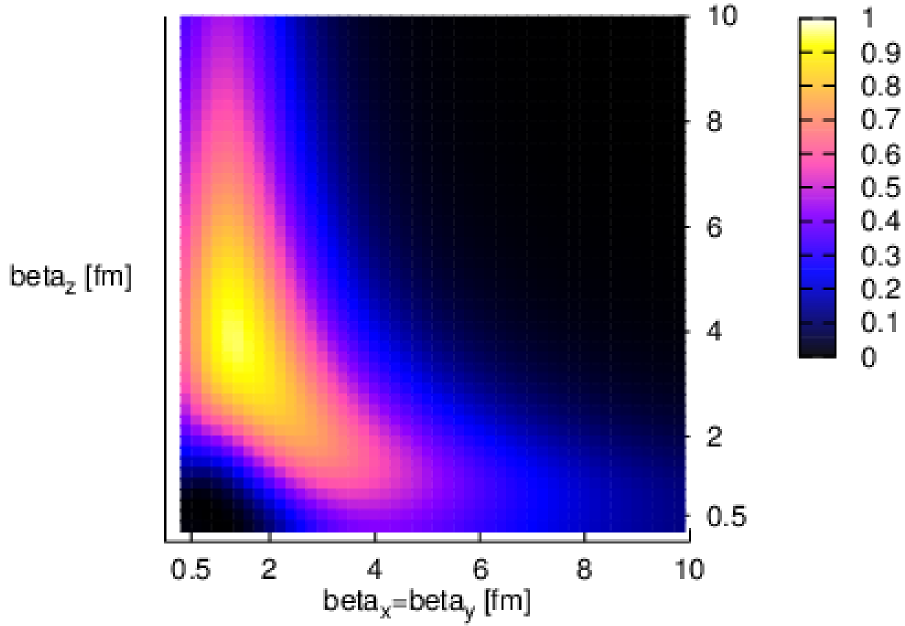

# 1 dim.-like linear-chain band

$0_3^+$

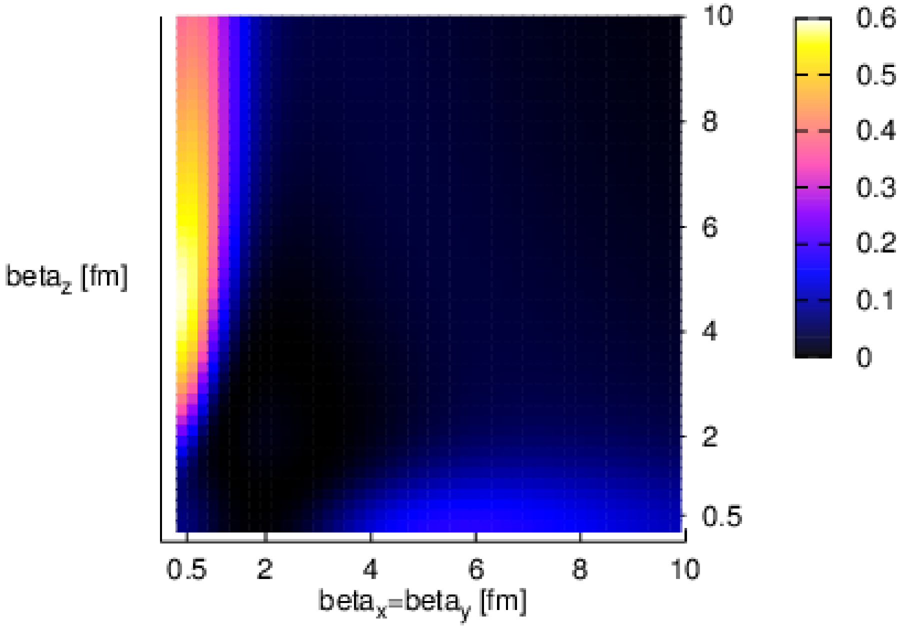


$2_3^+$

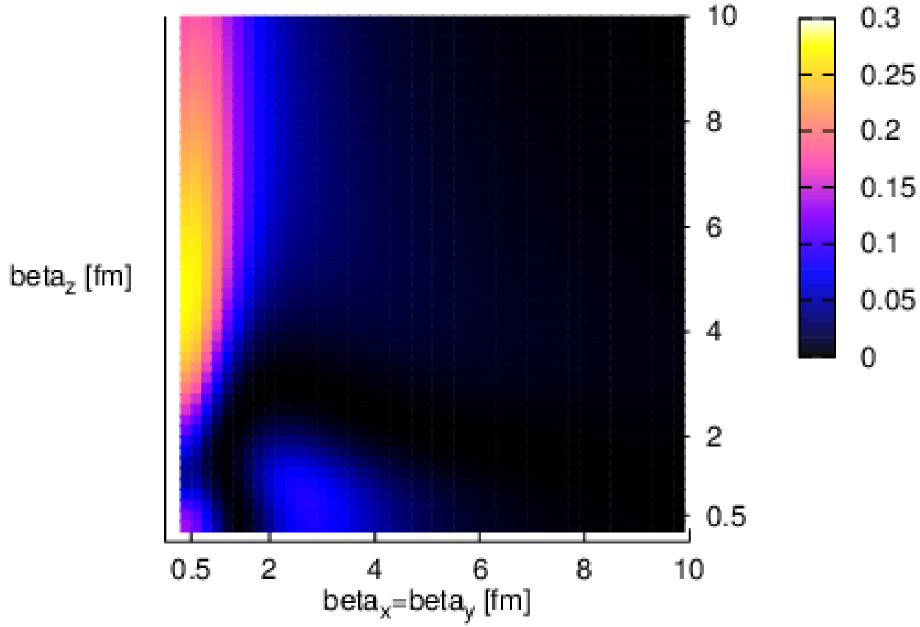


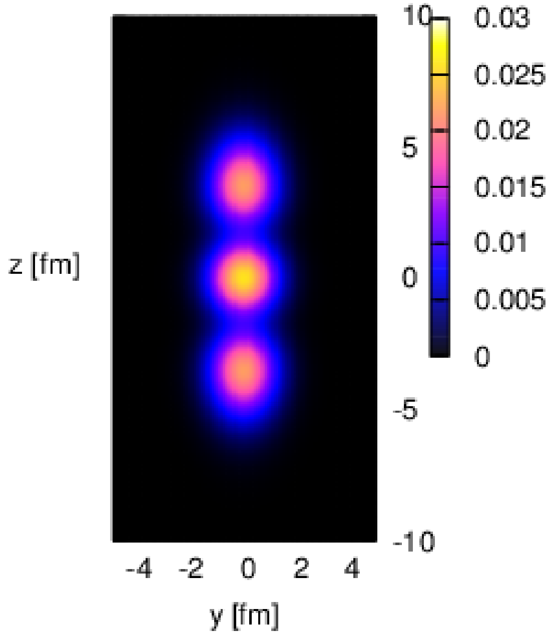

## Summary

- THSR w.f. gives nice description for gas-like states ($^{8}$Be, $^{12}$C, $^{16}$O) and even for ordinary cluster states ($^{20}$Ne and g.s. $^{12}$C)

  Common feature : Almost 100 % squared overlap with single THSR w.f.

  Container (mean-field-like) picture from gas-like to non-gas-like states

- Fully microscopic Hyper-THSR w.f.

  very promising way of describing light Λ hypernuclei

  shrinkage effect can be properly considered.

  non-gas-like Hoyle state (rmsr: 2.8 fm)

  one dimensional linear chain state

# Thanks

## to my Collaborators

*Bo Zhou (Nanjing U., RIKEN)*

*Zhongzhou Ren (Nanjing U.)*

*Chang Xu (Nanjing U.)*

*Taiichi Yamada (Kanto Gakuin U.)*

*Hisashi Horiuchi (RCNP)*

*Akihiro Tohsaki (RCNP)*

*Peter Schuck (IPN, Orsay)*

*Gerd Röpke (Rostock U.)*

*Shigeo Ohkubo (Kochi women U.)*

*Emiko Hiyama (RIKEN)*

*Kiyomi Ikeda (RIKEN)*

## and for your attention.

# 1 dim. Linear-chain intrinsic shape from THSR

(0.01 fm, 5.1 fm) での3-alpha THSR w.f.

1dim. Brink w.f. の重ね合わせ解 ($0^+$)と98.7 % 一致。

with T. Suhara, H. Horiuchi

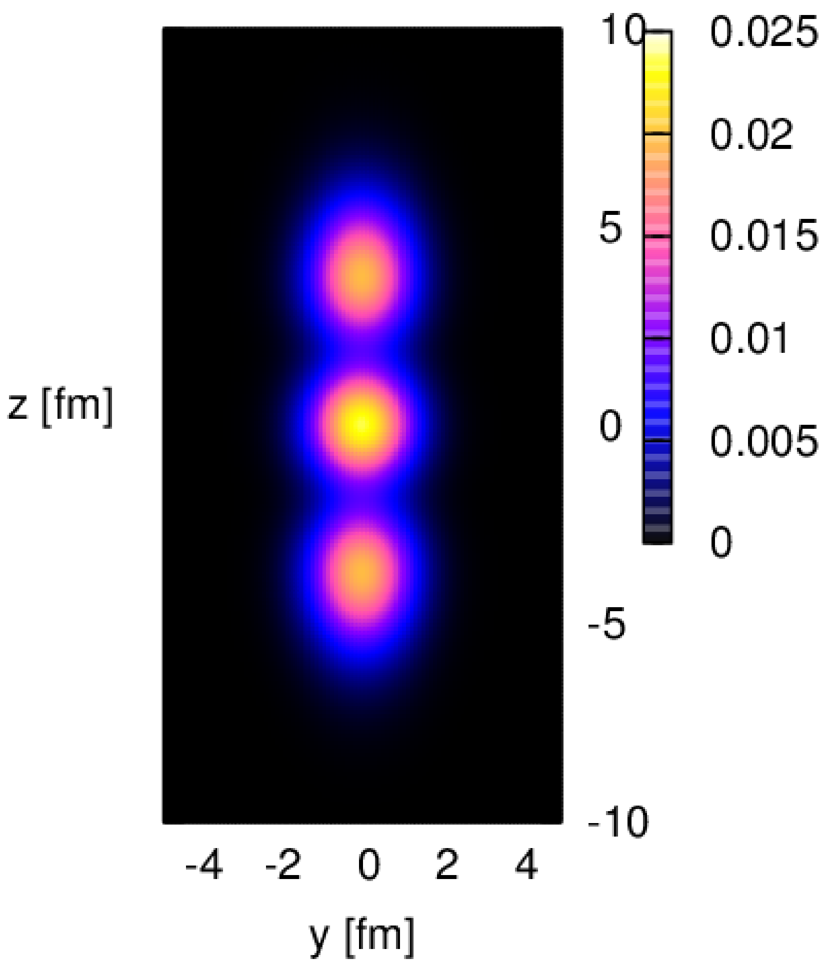


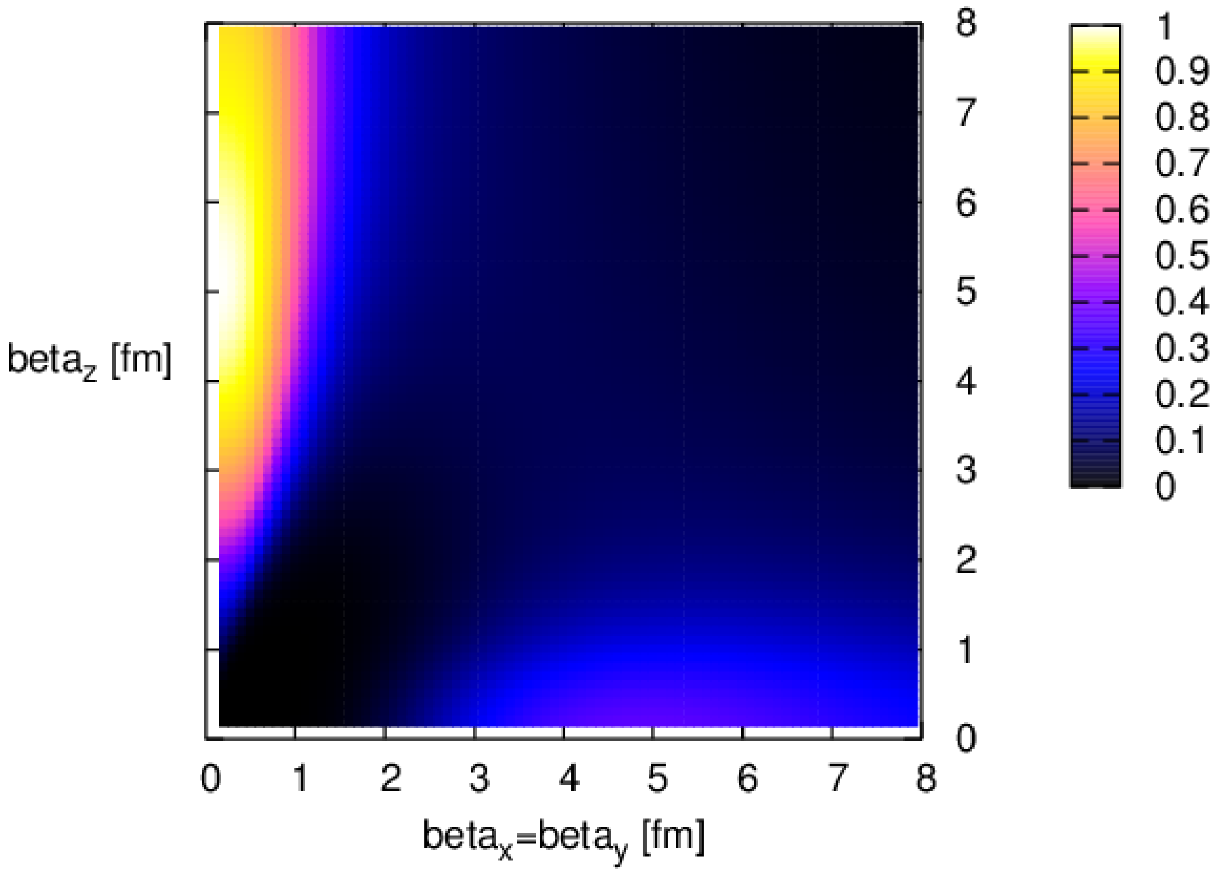

# Energy surface in orthogonal space to the g.s. and Hoyle

$$E(\beta_\perp, \beta_z) = \frac{\left\langle \hat{\mathcal{P}}^{\perp}_{\text{g.s.,Hoyle}} \, \Phi^{\text{THSR}}_{J=0}(B_\perp, B_z) \middle| H \middle| \hat{\mathcal{P}}^{\perp}_{\text{g.s.,Hoyle}} \, \Phi^{\text{THSR}}_{J=0}(B_\perp, B_z) \right\rangle}{\left\langle \hat{\mathcal{P}}^{\perp}_{\text{g.s.,Hoyle}} \, \Phi^{\text{THSR}}_{J=0}(B_\perp, B_z) \middle| \hat{\mathcal{P}}^{\perp}_{\text{g.s.,Hoyle}} \, \Phi^{\text{THSR}}_{J=0}(B_\perp, B_z) \right\rangle}$$

$E^{\text{thr.}}_{3\alpha} = -82.04$ MeV

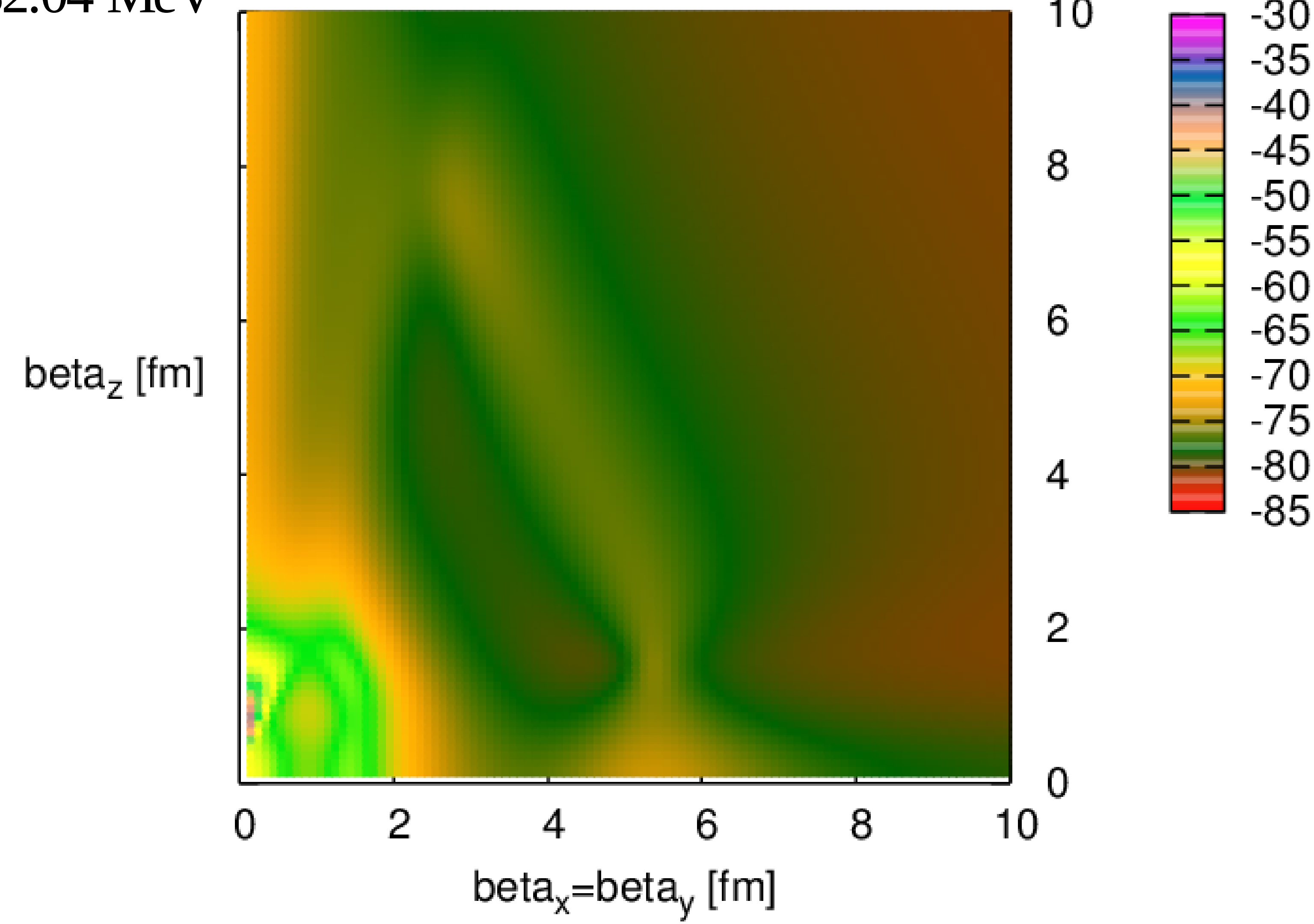

*Hint of how to improve the THSR w.f. to contain alpha+$^{16}$O structures*

*Y. F. et al., PRC82, 024312 (2010).*

## $^{16}$O

**GCM with 4α THSR w.f.**

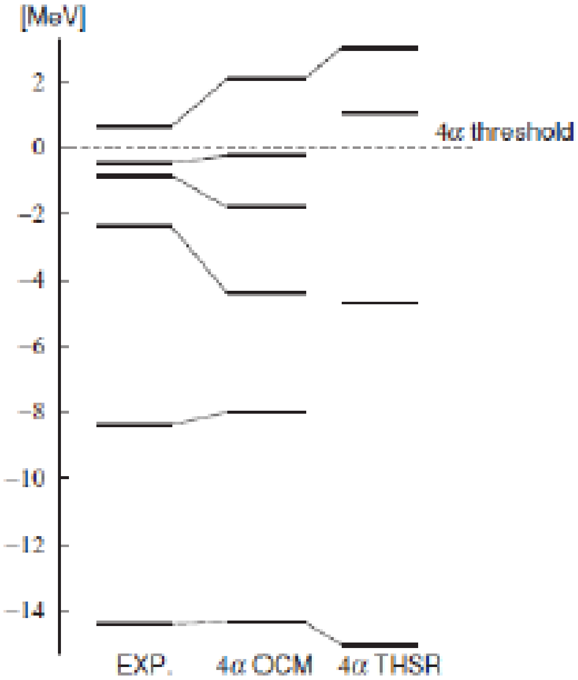


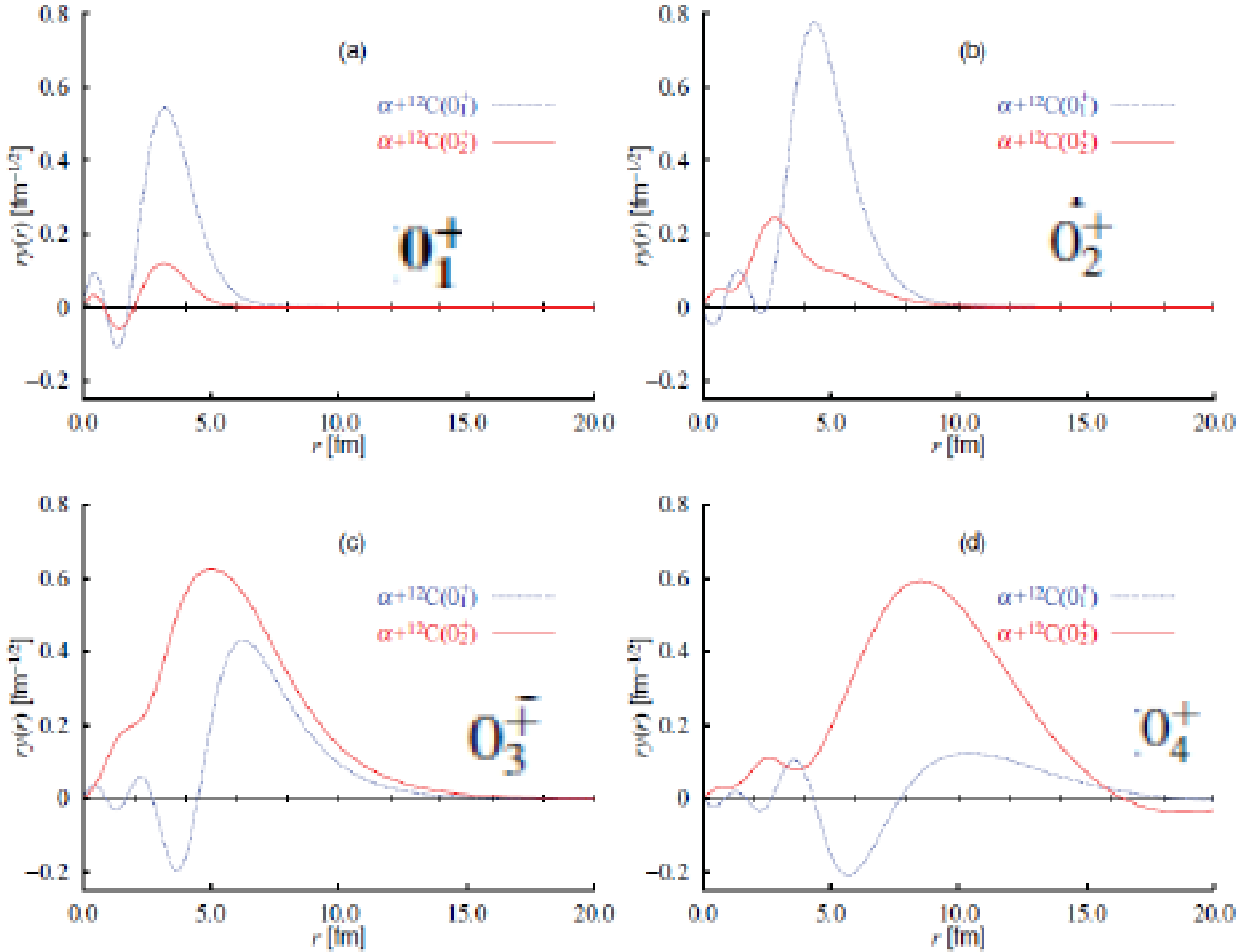


FIG. 6. (Color online) RWAs $r\mathcal{Y}_{L=0}(r)$ defined by Eq. (18) for the (a) $(0_1^+)_{THSR}$, (b) $(0_2^+)_{THSR}$, (c) $(0_3^+)_{THSR}$, and (d) $(0_4^+)_{THSR}$ states in two channels $\alpha + {}^{12}C(0_1^+)$ (dotted curve) and $\alpha + {}^{12}C(0_2^+)$ (solid curve).

**GCM calculation with respect to *B*-parameter.**